SUPPLEMENTARY METHODS

Patients

The Suppression of Ovarian Function Trial (SOFT) is a multicenter, randomised, open label, phase III trial in which 3,066 premenopausal women with hormone receptor-positive early breast cancer were randomly assigned in a 1:1:1 ratio to adjuvant endocrine therapy with tamoxifen alone (20 mg orally daily), tamoxifen plus ovarian suppression, or exemestane (25 mg orally daily) plus ovarian suppression for 5 years. Randomization was stratified according to use of prior chemotherapy, lymph-node status, and intended initial method of ovarian function suppression (if randomly assigned to OFS). Ovarian function suppression was achieved by the choice of gonadotropin-releasing hormone agonist triptorelin (3.75 mg intramuscular injection every 28 days), bilateral oophorectomy, or bilateral ovarian irradiation. Details of the study have been previously reported after a median follow up of 5.6 years,[1] and subsequently after a median follow up of 8 years,[2] and after a median follow up of 12 years.[3] Participants required documented premenopausal status, operable invasive breast cancer, and tumours that expressed estrogen and/or progesterone receptors in at least 10% of cells according to local assessment to be eligible. The SOFT trial is registered with ClinicalTrials.gov, number NCT00066690. The ethics committees and required health authorities of each participating center approved the trial protocols, and all patients provided written informed consent. Tumour and normal FFPE tissue blocks were prospectively collected and patients consented for protocol-mandated central review of histopathologic features and expression of ER, PgR, HER2, and Ki-67 labeling index,[4] with optional banking of FFPE tissue for future research at time of initial consent. The IBCSG Biological Project Working Group approved this investigation.

The study workflow is shown in Supp Figure 1 including reasons for patient sample exclusion. There were 1744 patients who had adequate consent for future research of submitted FFPE tumor blocks from which DNA was successfully extracted. 1,509 patient tumour samples were selected for targeted DNA-sequencing after exclusions for HER2-positive results by central or local assessment. A smaller young-age, case-control subsample were selected for whole-exome sequencing. Patients in this subsample were selected using a matched case-control design and included 47 patients who had a distant recurrence event (by 5 years median follow up in the entire study population), and 47 controls that were individually matched by age at randomization (within 8 years), nodal status (positive vs negative), tumour size (<2 cm vs ≥2 cm), local assessment of tumor grade (1, 2, 3), estrogen receptor expression as measured centrally if available or locally otherwise (<50% vs ≥50%), and treatment assignment.

DNA extraction

DNA was extracted from samples, all of which were derived from formalin-fixed, paraffin-embedded tumour tissue from primary breast cancers. For whole-exome sequencing, matched normal DNA was extracted from adjacent normal tissue. DNA was quantified with the dsDNA HS Assay kit (Qubit) with a minimum quantity of 200 ng required. Macrodissection was performed in cases with lower tumour cellularity.

Targeted DNA-sequencing

We performed targeted DNA-sequencing using a customized hybridisation capture panel designed specifically for recurrent breast cancer genes using the Agilent SureSelectXT Target Enrichment System. A list of target genes is shown on table 1 at https://breast-cancer-research.biomedcentral.com/articles/10.1186/s13058-020-01328-0#Sec2.[5]

DNA from each sample was fragmented using ultrasonification (Covaris Inc., USA), and libraries were prepared using the KAPA Hyper Prep Kit (KAPA Biosystems, USA). Libraries that passed quality control underwent hybridisation capture with custom RNA baits utilising the Bravo automated liquid handling robot (Agilent Technologies, Australia). Successfully captured libraries were indexed and pooled, then underwent paired end sequencing on the Illumina MiSeq or NextSeq.

Samples were required to have a mean coverage of 80X or greater for target regions to be eligible for further analysis. Of the 1,509 patient tumour samples that were selected for targeted DNA-sequencing, 1,292 (86%) successfully completed targeted sequencing. After further exclusions (non-inclusion in the intention-to-treat population [N=3], central HER2-positive on second review [N=14], triple negative breast cancer (ER and PgR absent) on central review [N=17]), 1,258 (83%) samples were evaluable for the analysis.

Raw paired end reads underwent adapter trimming with cutadapt (v1.7.1).[6] The sequencing reads were then aligned to the full hg19 genomic assembly using bwa mem (v0.7.13) with default settings.[7] Sequencing reads with mapping quality < 20 were filtered using SAMtools (v1.4.1).[8] Duplicate reads were removed using Picard tools (v1.119).[9] Indel realignment and base recalibration was performed using GATK (v3.8).[10] Variant calling of substitutions, insertions, and deletions was performed using VarDict (v1.5.1) in single sample mode with default settings.[11] Variants called by VarDict were then filtered using the filter parameter 'PASS'. Further filters were applied based on variant type: single nucleotide variants were filtered if they had <5 supporting reads or a total sequencing depth of < 30 reads; insertions and deletions were filtered if they had < 10 supporting reads or a total sequencing depth of < 50 reads. The subsequent variants were then annotated using ANNOVAR (dated 2018-04-

16).[12] Variants were further filtered if they were present in 3 or more samples from a pool of 23 process-matched normals or had a population allele frequency of ≥ 0.001 in the 1000 Genomes Project (August 2015).[13] In order to further reduce false positives, a final filter of variants with allele-frequency < 0.05 or variants with supporting reads ≤ 10 was performed. Oncogenic status of variants was then annotated using OncoKB (downloaded 23.05.19)[14] and Cancer Hotspots.[15] Variants that were annotated as "Oncogenic" or "Likely Oncogenic" using OncoKB, or were annotated as a cancer hotspot (q value < 0.05) were retained for analysis of driver variants.

For copy number analysis, copy number ratios for each tumour sample were attained using CNVkit (v0.9.3) with a reference of a pool of 23 process-matched normal, using default settings.[16] Copy number ratios then underwent winsorization using the R package "copynumber".[17] Segmentation was then performed using circular binary segmentation in the CNVkit package. Focal gene copy number status was determined based on segmentation results. A mean log ratio ≥ 0.8 was considered to be amplified, and a mean log ratio of < -0.8 was considered to indicate a homozygous deletion. Oncogenic status of the amplifications or deletions was annotated using OncoKB (downloaded 23.05.19),[14] with only copy number alterations annotated as "Oncogenic" or "Likely Oncogenic" retained for analysis of driver variants.

Approach to copy number analysis

The approach to calling copy number using off-target reads was validated for the targeted panel assay using FISH assays for FGFR1 in 8 samples (Supp Methods Figure 1). The Log ratio was calculated from the total copy number FISH result. There was strong correlation between methods (Pearson's product-moment correlation 0.90, p.value = 0.0024).

Supp Methods Figure 1: Correlation between log ratio from sequencing and FISH.

The relationship between log ratio and the true copy number state of the tumour is influenced by the purity of the sample and the ploidy. It is not possible to determine these variables for each sample using read depth copy number approaches alone as have been employed. Selection of appropriate log ratio cut-offs to call copy number amplifications or deletions therefore poses a challenge. Simulation of various combinations of ploidy and purity were performed (Supp Methods Figure 2). Here, the expected log ratio of a gene LR_g is calculated from the copy number of the gene CN_g, the tumour ploidy equivalent to whole genome copy number CN_w and the tumour purity p:

$$LR_g = log2\left(\frac{\left(p \times CN_g\right) + \left((1-p) \times 2\right)}{\left(p \times CN_w\right) + \left((1-p) \times 2\right)}\right)$$

This is an oversimplification, not accounting for subclonality, and also assumes that there is a linear relationship between the amount of DNA from a genomic region and the sequenced read depth in that region. Supp Methods Figure 2 shows that there is no single cut-off which performs well in all scenarios. However, taking into account that lower ploidies are more common, breast tumour samples are rarely highly pure and accuracy for calling amplifications is a priority over deletions as they are more likely to be targetable, a log ratio of ≥ 0.8 for amplifications and ≤ -0.8 for deletions was chosen. The relationship between derived copy number and tumour purity for these cut-offs at various ploidies is shown in Supp Methods Figure 3. This highlights that purity has a significant impact on the detection of significant amplifications and alterations, and the inability to estimate purity using read depth copy number methods is therefore an important limitation. These plots also show that the minimum magnitude of a copy number alteration may be estimated by calculating the total copy number from the log ratio assuming a completely pure tumour.

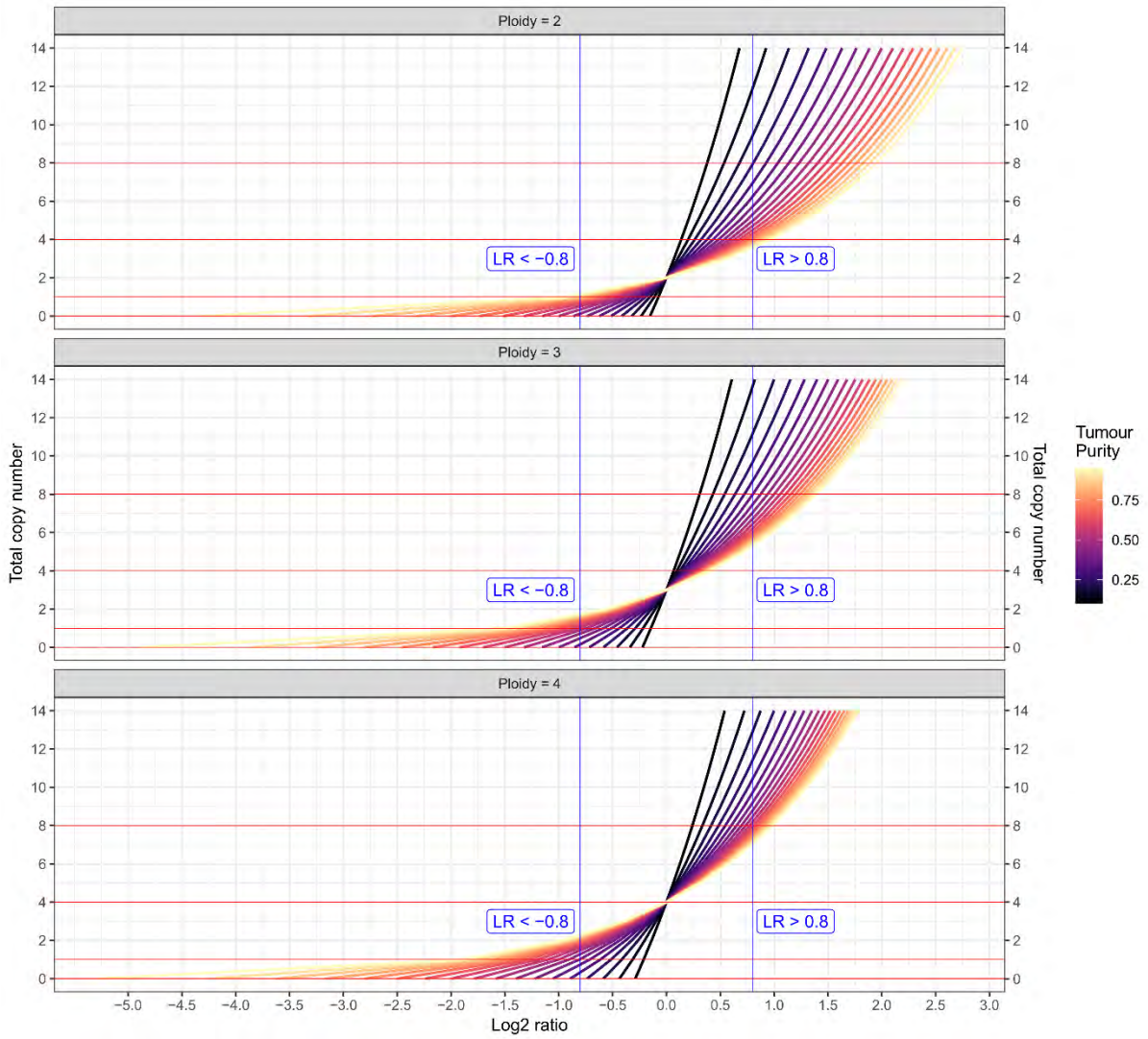

Supp Methods Figure 2: Simulated copy number data showing effect of different purity and ploidy.

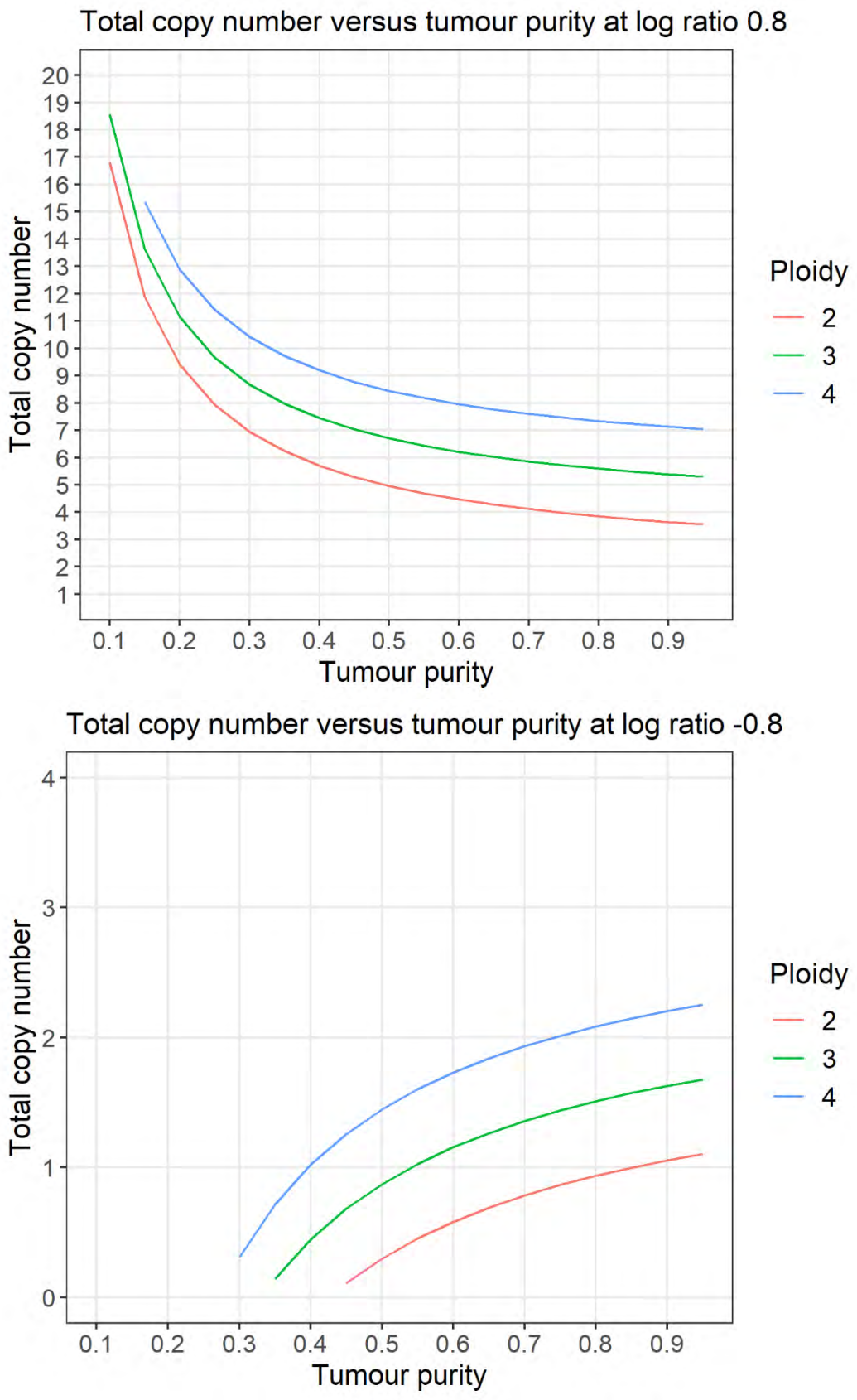

Supp Methods Figure 3: Total copy number at LR 0.8 (top) and -0.8 (bottom) at different ploidy and purity.

Whole-exome sequencing

We performed targeted whole-exome sequencing using the Agilent SureSelect DNA – SureSelect Human All Exon V6 r2 kit. DNA from each sample was fragmented using ultrasonification (Covaris Inc., USA), and libraries were prepared using the KAPA Hyper Prep Kit (KAPA Biosystems, USA). Libraries that passed quality control underwent hybridisation capture using the previously mentioned Agilent whole-exome sequencing kit with the Bravo automated liquid handling robot (Agilent Technologies, Australia). Successfully captured libraries were indexed and pooled, then underwent paired end sequencing on the Illumina MiSeq or NextSeq.

The design planned 100 patients (50 matched case-controls) to have paired tumor and normal samples analysed by whole exome sequencing. Of the 94 patients' pairs of tumour and normal samples that underwent whole-exome sequencing, 12 patients' samples were unsuccessful, as 7 failed to be sequenced due to unsuccessful library preparation or capture, and 5 had tumour samples that were unsuccessful due to inadequate depth of coverage (< 70X for target regions) and in which there was no supporting targeted sequencing available. Thus 82 of 94 patients had successful WES, of which 73 (78%) had tumour/normal pairs successfully sequenced, and 9 (10%) had tumour samples successfully sequenced but without the normal sample. With exclusion of 12 patients' tumour/normal samples that failed sequencing, there was 1 matched case-control set lost and 10 (6 cases and 4 controls) in which case-control matching was broken. A further matching step was performed for the broken case-controls, resulting in one new matched case-control set, and 8 case-control groups of 3 patients with 2:1 or 1:2 matches.

Raw paired end reads underwent adapter trimming with cutadapt (v1.7.1).[6] The sequencing reads were then aligned to the full hg19 genomic assembly using bwa mem (v0.7.13) with

default settings.[7] Sequencing reads with mapping quality < 20 were filtered using SAMtools (v1.4.1).[8] Duplicate reads were removed using Picard tools (v1.119).[9] Indel realignment and base recalibration was performed using GATK (v3.8).[10] Variant calling of substitutions, insertions, and deletions was performed using Mutect2 (v3.8-0) in tumour-normal mode for tumour/normal pairs, and in tumour-only mode for tumours without paired normal samples with default settings.[18,19] Variants called by Mutect2 were then filtered using the filter parameter 'PASS'. For variants from tumour/normal pairs, further filters were applied based on variant type: single nucleotide variants were filtered if they had < 5 supporting reads in the tumour or ≥ 5 supporting reads in the normal or a total sequencing depth of < 30 reads; insertions and deletions were filtered if they had < 10 supporting reads in the tumour or ≥ 5 supporting reads in the normal or a total sequencing depth of < 50 reads. For variants from tumour samples without paired normal samples, further filters were applied based on variant type: single nucleotide variants were filtered if they had < 5 supporting reads in the tumour or a total sequencing depth of < 30 reads; insertions and deletions were filtered if they had < 10 supporting reads in the tumour or a total sequencing depth of < 50 reads. The subsequent variants were then annotated using ANNOVAR (dated 2018-04-16).[12] Variants were further filtered if they were present in 3 or more samples from a pool of 73 process-matched normals or had a population allele frequency of ≥ 0.001 in the 1000 Genomes Project (August 2015).[13] In order to further reduce false positives, a final filter of variants with allele-frequency < 0.05 or variants with supporting reads ≤ 10 was performed. Oncogenic status of variants was then annotated using OncoKB (downloaded 23.05.19)[14] and Cancer Hotspots.[15] Variants that were annotated as "Oncogenic" or "Likely Oncogenic" using OncoKB, or were annotated as a cancer hotspot (q value < 0.05) were retained for analysis of driver variants.

For allele-specific copy number analysis of tumour/normal pairs we used the FACETS algorithm (v0.5.14) to estimate tumour purity, ploidy, and allele-specific integer copy number.[20] An initial low-sensitivity run (cval=150) was first used to determine the diploid tumour-normal log-ratio value and purity. A second run (cval=100) was then used to infer allele-specific copy number data. For allele-specific copy number analysis of unmatched tumour samples we used the PureCN algorithm (v1.14.1) with a pool of 73 process-matched normals to estimate tumour purity, ploidy, and allele-specific integer copy number.[21] Focal gene copy number status was determined based on segmentation results. An estimated integer copy number ≥ 2*ploidy+1 was considered to represent amplification. An estimated integer copy number of 0 was considered to represent homozygous deletion, and an estimated integer copy number of 1 was considered to represent loss of heterozygosity. Oncogenic status of the amplifications or deletions was annotated using OncoKB (downloaded 23.05.19),[14] with only copy number alterations annotated as "Oncogenic" or "Likely Oncogenic" retained for analysis of driver variants.

Integrated cluster validation

Integrated clusters have been defined in previously reported large analyses which define 10 classifications based on clustering using a combination of copy number and transcriptomic profiles from early breast cancers.[22,23] Most of these clusters were defined by specific characteristic copy number aberrations.[24] In the absence of gene expression data from our dataset, we sought to validate the prognostic utility of this classification using a simplified system based solely on the presence or absence of these characteristic copy number aberrations. The following focal gene copy number aberrations were used to classify IntClust groups that were prevalent in hormone receptor-positive, HER2-negative early breast cancers.

- IntClust 1 – amplifications of *HSF5*, *PPM1E*, *PRR11*, *DHX40*, *TUBD1*, *RPS6KB1*, *CA4*, *C17orf64*, *BCAS3*, *TBX2*, *BRIP1*, *TBC1D3P2*.
- IntClust 2 – amplifications of *FGF3*, *CCND1*, *CTTN*, *OMP*, *PAK1*, *RSF1*, *NARS2*.
- IntClust 6 – amplifications of *ZNF703*, *EIF4EBP1*, *LETM2*, *STAR*, *FGFR1*.
- IntClust 9 – amplifications of *FBXO32*, *SQLE*, *LINC00861*, *PCAT1*, *MYC*, *LINC00977*, *MIR5194*, *ADCY8*.

There were samples that contained characteristic copy number aberrations of more than one IntClust group. Such tumours with amplifications in multiple amplicons were classified as "multiple amplifications". Conversely, there were samples that contained none of the characteristic copy number aberrations and were classified as "amplification-devoid". The remainder of tumours contained copy number aberrations of only one IntClust group and were classified as the respective amplicon and IntClust-like category.

Genomic features and mutational signatures

Evaluation of whole genome integrity index (wGII) and whole genome doubling was performed using previously described methods on allele specific copy number data from all samples from the young-age, case-control subsample that had undergone WES (N=82 samples).[25,26] Mutational signatures were assessed in the young-age, case-control subsample that had successful WES of tumour/normal sample pairs (N=73 patients' samples), using the 'deconstructSigs' package.[27] Normalisation was performed with the "tri.counts.method" parameter set as "exome", and assigned only to COSMIC signatures that are known to be present in breast cancers (signature 1, 2, 3, 5, 8, 13, 17, 18).

Mutational signature 3 was further assessed using the SigMA tool,[28] which is optimised to detect mutational signature 3 in next generation sequencing variant calls that has utilised whole

exome sequencing or large capture panels. SigMA was run using “seqcap_probe” for the data parameter and “breast” for the tumour type parameter.

Homologous recombination deficiency

The presence of features of homologous recombination deficiency (HRD) was evaluated in all tumour/normal samples in the young-age, case-control subsample that had successful WES of tumour/normal sample pairs (N=73 patients’ samples) using HRDetect modified for WES (here termed eHRDetect). We adapted the previously developed HRDetect model[29] for whole exome sequencing (WES) data. The model was trained on 640 breast cancers, down-sampled to represent the equivalent of a WES experiment. To estimate the activities (exposures) of mutational signatures in the samples, COSMIC mutational signatures relevant to breast cancers were converted according to exome trinucleotide frequencies (substitution signatures 1, 2, 3, 5, 6, 8, 13, 17, 18, 20, 26). Mutational signatures were fitted using non-negative least squares (NNLS), which performs better than KL-divergence (KLD), possibly because of the sparsity of exome catalogues. Indels were classified as usually performed in whole genome sequencing data. Before training, features were log transformed and standardized (as in Davies et al. 2017). We trained a logistic regression classifier using only substitution signatures 3 and 8 and the count of deletions with microhomology at the indel junction. The model coefficients were 2.94, 0.53 and 0.62 respectively with a cut-off for HRDetect high versus low of 0.35. The WES HRD classifier here relies heavily on substitution signature 3 which may lead to a higher false positive rate.

Five tumour/normal paired samples were not evaluable due to low number of mutations. An eHRDetect score of > 0.7 was classified as positive, and ≤ 0.7 was classified as negative.

The presence of genetic alterations in HRD-related genes was also evaluated in the combined sequencing cohort. This included “Oncogenic” or “Likely Oncogenic” genetic alterations in the following HRD-related genes which were obtained from a previously reported clinical trial of metastatic breast cancer patients with the use of olaparib:[30]

- *BRCA1*
- *BRCA2*
- *PALB2*
- *ATM*
- *CHEK2*
- *BLM*
- *BARD1*
- *RAD50*
- *BRIP1*
- *FANCA*

TCGA-Breast cancer dataset

Publicly available clinical and genomic data from the TCGA-BRCA was used for validation purposes.[31] Data was downloaded from the Genomics Data Commons Data Portal (https://portal.gdc.cancer.gov/). The file “TCGA.BRCA.mutect.995c0111-d90b-4140-bee7-3845436c3b42.DR-10.0.somatic.maf.gz” was used for short variants and the file “BRCA_focal_score_by_genes.txt” was used for copy number alterations.

Tumours were considered to be hormone receptor-positive and HER2-negative as per ASCO-CAP guidelines. Patients were considered to be postmenopausal at diagnosis if they were

annotated as “postmenopausal” in the TCGA-Breast data, or if they were > 55 years of age at diagnosis if they were annotated as having an unknown menopausal status.

BIG 1-98 trial

Clinical and genomic data from a secondary analysis of the BIG 1-98 clinical trial were used for validation purposes and for comparisons between pre-menopausal and post-menopausal populations. BIG 1-98 was a randomised, double-blind, phase 3 trial that included only post-menopausal patients with hormone receptor-positive, operable, invasive early breast cancer.[32-34] Patients were randomized to monotherapy with letrozole, tamoxifen, or a sequential endocrine strategy with the 2 agents for 5 years. The BIG 1-98 trial is registered with ClinicalTrials.gov, number NCT00004205. The secondary analysis included 538 participants selected in a case-cohort-like design (case being a distant recurrence), in which the patient’s tumours underwent targeted DNA sequencing using Foundation Medicine’s T5-targed panel of 287 known cancer genes, and has been previously reported.[35]

Tumor-infiltrating lymphocytes

Tumour-infiltrating lymphocyte (TIL) levels have been previously shown to be generally low in HR+HER2- early breast cancers.[36,37] Therefore, only selected groups of interest were evaluated for TILs. Namely, the young-age, case-control subsample, and the samples with ER-expression of < 50% by immunohistochemistry.

Quantification of stromal tumour-infiltrating lymphocytes was evaluated from haematoxylin and eosin stained sections of tumour samples using our previously published methodologys.[38,39] In brief, quantification of tumour-infiltrating lymphocytes in the tumour stroma was recorded as a percentage of the occupied stromal areas. A freely available website

describing the method can be found along with a training tool for tumour-infiltrating lymphocyte assessment by pathologists (www.tilsinbreastcancer.org).

Validation of TIL findings was performed using publicly available data from a previously reported pan-cancer TCGA analysis using the variable "til_percentage".[40]

Statistical analysis

The combined sequencing cohort includes all patients with tumour samples that successfully underwent DNA sequencing of any type (N=1,276). The young-age, case-control subsample includes only patients <45 years that underwent successful whole-exome sequencing of both tumor/normal or only tumor (N=82); 64/82 patients had both targeted sequencing and WES. Luminal-like status was defined using previously published St. Gallen consensus guidelines using centrally-determined ER, PR, and Ki-67 expression levels by immunohistochemistry as previously reported.[4,41]

For comparisons between genomic subgroups of patients within the SOFT combined sequencing cohort, categorical variables were analysed using the chi-squared tests, and continuous variables were analysed using t-tests for normally distributed variables, and the Mann-Whitney Wilcoxon tests for non-normally distributed variables. Driver alterations were defined as present or absent. For comparisons in driver alteration frequency between subgroups of patients, *P* values that were generated were subjected to multiple testing correction using the false discovery method.

For analysis of time-to-event endpoints, the primary end point was distant recurrence-free interval (DRFI), defined as the time from randomization to recurrence at a distant site. In

patients without a distant recurrence, censoring occurred at the date of last follow-up or death. The secondary end point was overall survival (OS), defined as the time from randomization to death from any cause, or was censored at the date last known alive. Cox proportional hazards regression models were used to analyse for associations with time-to-event endpoints. For association of driver alterations with endpoints, patients with the presence of the driver alteration were compared with patients without the driver alteration. For association of copy number altered subgroups with endpoints, each copy number altered subgroup was compared with patient subgroups that were classified as “amplification-devoid”. For association with genomic subgroupings with endpoints, each genomic subgroup was compared with the subgroup with “no poor prognostic features”. Unless otherwise stated in the text, all Cox models were stratified by nodal status and (neo)adjuvant chemotherapy receipt (no chemotherapy; prior chemotherapy and lymph node negative; prior chemotherapy and lymph node positive), and adjusted by treatment assignment. Hazard ratios with 95% confidence intervals were estimated and Wald tests were used, with a 2-sided value of $P < 0.05$ deemed to be statistically significant. The 8-year time-to-event estimates were calculated using the Kaplan-Meier method. Kaplan Meier curves were generated for visualization purposes.

We tested for significantly different associations of driver alterations with endpoints in very young women (< 40 years of age at randomization) compared with young women (≥ 40 years of age at randomization). To test for this, we added a product interaction term into a Cox proportional hazards regression model. The Wald test was used for significance, and we deemed a 2-sided value of Interaction $P < 0.05$ to be statistically significant.

To analyse for association of HRDetect score (positive vs negative) with DRFI in the young-age, case-control subsample that underwent WES, a conditional logistic regression model was used, stratified by the case-control matching.

Supplementary Methods References

1 Francis, P. A. *et al.* Adjuvant ovarian suppression in premenopausal breast cancer. *N Engl J Med* **372**, 436-446, doi:10.1056/NEJMoa1412379 (2015).

2 Francis, P. A. *et al.* Tailoring Adjuvant Endocrine Therapy for Premenopausal Breast Cancer. *N Engl J Med*, doi:10.1056/NEJMoa1803164 (2018).

3 Francis, P. A. *et al.* Adjuvant Endocrine Therapy in Premenopausal Breast Cancer: 12-Year Results From SOFT. *J Clin Oncol*, JCO2201065, doi:10.1200/JCO.22.01065 (2022).

4 Regan, M. M. *et al.* Predictive value and clinical utility of centrally assessed ER, PgR, and Ki-67 to select adjuvant endocrine therapy for premenopausal women with hormone receptor-positive, HER2-negative early breast cancer: TEXT and SOFT trials. *Breast Cancer Res Treat* **154**, 275-286, doi:10.1007/s10549-015-3612-z (2015).

5 van Geelen, C. T. *et al.* Clinical implications of prospective genomic profiling of metastatic breast cancer patients. *Breast Cancer Res* **22**, 91, doi:10.1186/s13058-020-01328-0 (2020).

6 Martin, M. Cutadapt removes adapter sequences from high-throughput sequencing reads. *2011* **17**, 3, doi:10.14806/ej.17.1.200 (2011).

7 Li, H. & Durbin, R. Fast and accurate short read alignment with Burrows-Wheeler transform. *Bioinformatics* **25**, 1754-1760, doi:10.1093/bioinformatics/btp324 (2009).

8 Li, H. *et al.* The Sequence Alignment/Map format and SAMtools. *Bioinformatics* **25**, 2078-2079, doi:10.1093/bioinformatics/btp352 (2009).

9 Broad Institute. Picard Toolkit. *GitHub Repository* (2019).

10 McKenna, A. *et al.* The Genome Analysis Toolkit: a MapReduce framework for analyzing next-generation DNA sequencing data. *Genome Res* **20**, 1297-1303, doi:10.1101/gr.107524.110 (2010).

11 Lai, Z. *et al.* VarDict: a novel and versatile variant caller for next-generation sequencing in cancer research. *Nucleic Acids Res* **44**, e108, doi:10.1093/nar/gkw227 (2016).

12 Wang, K., Li, M. & Hakonarson, H. ANNOVAR: functional annotation of genetic variants from high-throughput sequencing data. *Nucleic Acids Res* **38**, e164, doi:10.1093/nar/gkq603 (2010).

13 Genomes Project, C. *et al.* An integrated map of genetic variation from 1,092 human genomes. *Nature* **491**, 56-65, doi:10.1038/nature11632 (2012).

14 Chakravarty, D. *et al.* OncoKB: A Precision Oncology Knowledge Base. *JCO Precis Oncol* **2017**, doi:10.1200/PO.17.00011 (2017).

15 Chang, M. T. *et al.* Accelerating Discovery of Functional Mutant Alleles in Cancer. *Cancer Discov* **8**, 174-183, doi:10.1158/2159-8290.CD-17-0321 (2018).

16 Talevich, E., Shain, A. H., Botton, T. & Bastian, B. C. CNVkit: Genome-Wide Copy Number Detection and Visualization from Targeted DNA Sequencing. *PLoS Comput Biol* **12**, e1004873, doi:10.1371/journal.pcbi.1004873 (2016).

17 Nilsen, G. *et al.* Copynumber: Efficient algorithms for single- and multi-track copy number segmentation. *BMC Genomics* **13**, 591, doi:10.1186/1471-2164-13-591 (2012).

18 Benjamin, D. *et al.* Calling Somatic SNVs and Indels with Mutect2. *bioRxiv*, 861054, doi:10.1101/861054 (2019).

19 Cibulskis, K. *et al.* Sensitive detection of somatic point mutations in impure and heterogeneous cancer samples. *Nat Biotechnol* **31**, 213-219, doi:10.1038/nbt.2514 (2013).

20 Shen, R. & Seshan, V. FACETS: Allele-Specific Copy Number and Clonal Heterogeneity Analysis Tool Estimates for High-Throughput DNA Sequencing.
21 Riester, M. *et al.* PureCN: copy number calling and SNV classification using targeted short read sequencing. *Source Code Biol Med* **11**, 13, doi:10.1186/s13029-016-0060-z (2016).
22 Rueda, O. M. *et al.* Dynamics of breast-cancer relapse reveal late-recurring ER-positive genomic subgroups. *Nature* **567**, 399-404, doi:10.1038/s41586-019-1007-8 (2019).
23 Curtis, C. *et al.* The genomic and transcriptomic architecture of 2,000 breast tumours reveals novel subgroups. *Nature* **486**, 346-352, doi:10.1038/nature10983 (2012).
24 Dawson, S. J., Rueda, O. M., Aparicio, S. & Caldas, C. A new genome-driven integrated classification of breast cancer and its implications. *EMBO J* **32**, 617-628, doi:10.1038/emboj.2013.19 (2013).
25 Endesfelder, D. *et al.* Chromosomal instability selects gene copy-number variants encoding core regulators of proliferation in ER+ breast cancer. *Cancer Res* **74**, 4853-4863, doi:10.1158/0008-5472.CAN-13-2664 (2014).
26 Bielski, C. M. *et al.* Genome doubling shapes the evolution and prognosis of advanced cancers. *Nat Genet* **50**, 1189-1195, doi:10.1038/s41588-018-0165-1 (2018).
27 Rosenthal, R., McGranahan, N., Herrero, J., Taylor, B. S. & Swanton, C. deconstructSigs: delineating mutational processes in single tumors distinguishes DNA repair deficiencies and patterns of carcinoma evolution. *Genome Biol* **17**, 31, doi:10.1186/s13059-016-0893-4 (2016).
28 Gulhan, D. C., Lee, J. J., Melloni, G. E. M., Cortes-Ciriano, I. & Park, P. J. Detecting the mutational signature of homologous recombination deficiency in clinical samples. *Nat Genet* **51**, 912-919, doi:10.1038/s41588-019-0390-2 (2019).
29 Davies, H. *et al.* HRDetect is a predictor of BRCA1 and BRCA2 deficiency based on mutational signatures. *Nature Medicine* **23**, 517-525, doi:10.1038/nm.4292 (2017).
30 Tung, N. M. *et al.* TBCRC 048: A phase II study of olaparib monotherapy in metastatic breast cancer patients with germline or somatic mutations in DNA damage response (DDR) pathway genes (Olaparib Expanded). *Journal of Clinical Oncology* **38**, 1002-1002, doi:10.1200/JCO.2020.38.15_suppl.1002 (2020).
31 Cancer Genome Atlas, N. Comprehensive molecular portraits of human breast tumours. *Nature* **490**, 61-70, doi:10.1038/nature11412 (2012).
32 Breast International Group 1-98 Collaborative Group. A comparison of letrozole and tamoxifen in postmenopausal women with early breast cancer. *N Engl J Med* **353**, 2747-2757, doi:10.1056/NEJMoa052258 (2005).
33 B. I. G. Collaborative Group. Letrozole therapy alone or in sequence with tamoxifen in women with breast cancer. *N Engl J Med* **361**, 766-776, doi:10.1056/NEJMoa0810818 (2009).
34 Regan, M. M. *et al.* Assessment of letrozole and tamoxifen alone and in sequence for postmenopausal women with steroid hormone receptor-positive breast cancer: the BIG 1-98 randomised clinical trial at 8·1 years median follow-up. *The Lancet Oncology* **12**, 1101-1108, doi:10.1016/s1470-2045(11)70270-4 (2011).
35 Luen, S. J. *et al.* Association of Somatic Driver Alterations With Prognosis in Postmenopausal, Hormone Receptor-Positive, HER2-Negative Early Breast Cancer: A Secondary Analysis of the BIG 1-98 Randomized Clinical Trial. *JAMA Oncol*, doi:10.1001/jamaoncol.2018.1778 (2018).
36 Loi, S. *et al.* Prognostic and predictive value of tumor-infiltrating lymphocytes in a phase III randomized adjuvant breast cancer trial in node-positive breast cancer comparing the addition of docetaxel to doxorubicin with doxorubicin-based

chemotherapy: BIG 02-98. *J Clin Oncol* **31**, 860-867, doi:10.1200/JCO.2011.41.0902 (2013).
37 Denkert, C. *et al.* Tumour-infiltrating lymphocytes and prognosis in different subtypes of breast cancer: a pooled analysis of 3771 patients treated with neoadjuvant therapy. *Lancet Oncol* **19**, 40-50, doi:10.1016/S1470-2045(17)30904-X (2018).
38 Salgado, R. *et al.* The evaluation of tumor-infiltrating lymphocytes (TILs) in breast cancer: recommendations by an International TILs Working Group 2014. *Ann Oncol* **26**, 259-271, doi:10.1093/annonc/mdu450 (2015).
39 Dieci, M. V. *et al.* Update on tumor-infiltrating lymphocytes (TILs) in breast cancer, including recommendations to assess TILs in residual disease after neoadjuvant therapy and in carcinoma in situ: A report of the International Immuno-Oncology Biomarker Working Group on Breast Cancer. *Semin Cancer Biol* **52**, 16-25, doi:10.1016/j.semcancer.2017.10.003 (2018).
40 Saltz, J. *et al.* Spatial Organization and Molecular Correlation of Tumor-Infiltrating Lymphocytes Using Deep Learning on Pathology Images. *Cell Reports* **23**, 181-193.e187, doi:10.1016/j.celrep.2018.03.086 (2018).
41 Goldhirsch, A. *et al.* Personalizing the treatment of women with early breast cancer: highlights of the St Gallen International Expert Consensus on the Primary Therapy of Early Breast Cancer 2013. *Ann Oncol* **24**, 2206-2223, doi:10.1093/annonc/mdt303 (2013).

Supplementary Table 1

	< 40 years at diagnosis with HR+HER2- BC	< 35 years at diagnosis with HR+HER2- BC
TCGA-Breast	50	19
METABRIC	42	14
SOFT	359	123

Supplementary Table 1 - Table demonstrating the number of young, premenopausal patients with HR+HER2- early breast cancer within publicly available genomic databases.

Supplementary Figure 1

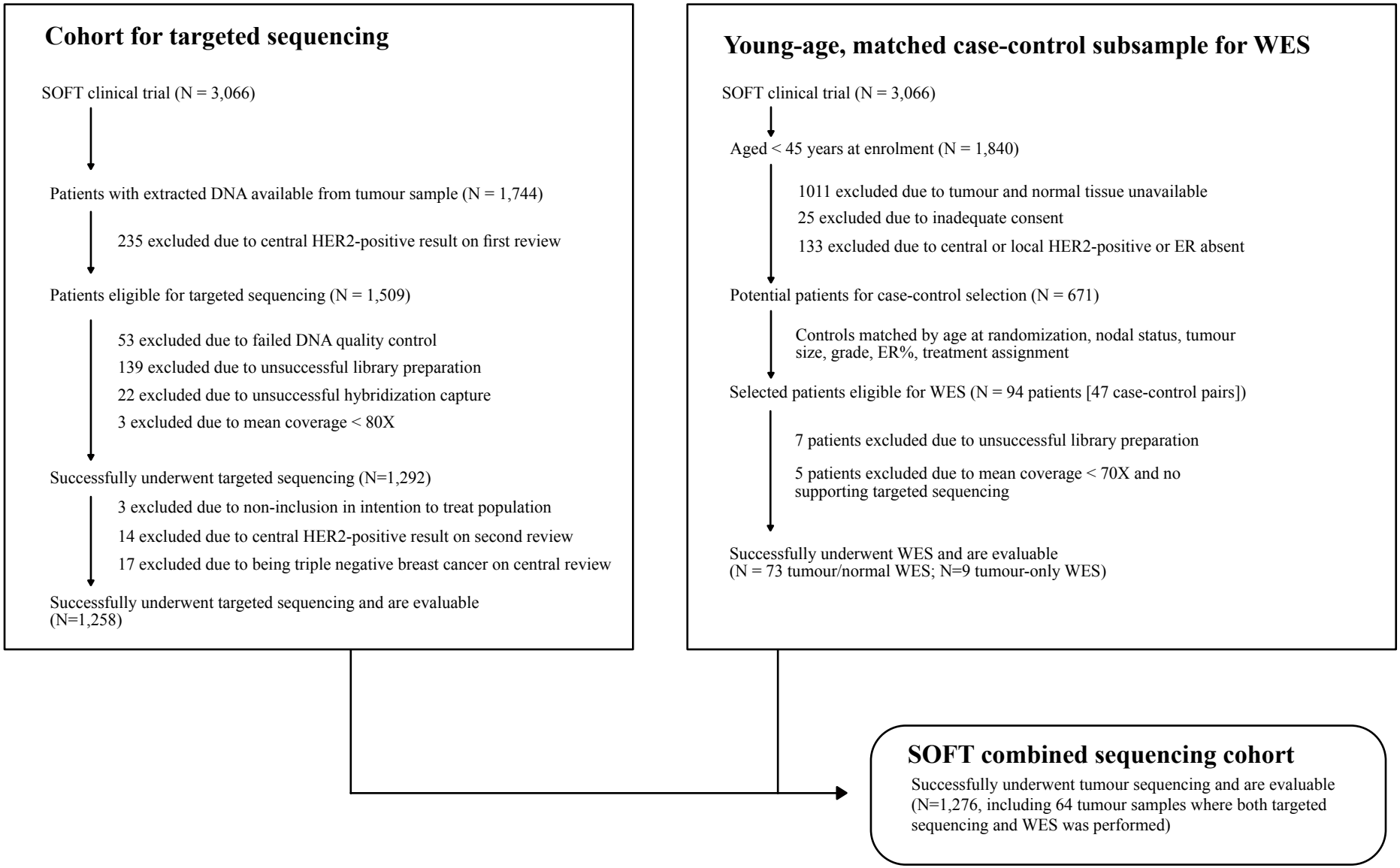

Supplementary Figure 1 - Study workflow demonstrating patient selection and cohorts for sequencing. Abbreviations: WES, whole exome sequencing.

Supplementary Table 2

Clinicopathological characteristics of the combined sequencing cohort			
	Sequencing cohort (N = 1,276)	**Entire SOFT cohort (N = 3,066)**	**Entire SOFT HER2-negative cohort (N = 2,643)**
Age at enrolment			
< 35 years	123 (10%)	351 (11%)	259 (10%)
35 - 39 years	236 (19%)	588 (19%)	486 (18%)
≥ 40 years	917 (72%)	2127 (69%)	1898 (72%)
Tumour size			
≤ 2 cm	833 (65%)	2021 (66%)	1798 (68%)
> 2 cm	422 (33%)	967 (32%)	789 (30%)
Unknown	21	78	56
Lymph node status			
Positive	431 (34%)	1055 (34%)	866 (33%)
Negative	842 (66%)	2011 (66%)	1777 (67%)
Unknown	3		
Tumour grade			
One	312 (25%)	715 (23%)	677 (26%)
Two	715 (56%)	1651 (54%)	1461 (55%)
Three	248 (19%)	669 (22%)	489 (19%)
Unknown	1	31	16
Estrogen receptor expression			
≥ 90%	1064 (83%)	2232 (73%)	1974 (75%)
< 90%	211 (17%)	793 (26%)	639 (24%)
Unknown	1	41	30
Progesterone receptor expression			
≥ 20%	1143 (90%)	2598 (85%)	2289 (87%)
< 20%	131 (10%)	422 (14%)	319 (12%)
Unknown	2	46	35
Ki-67 expression			
≥ 20%	452 (35%)	948 (31%)	740 (28%)
< 20%	788 (62%)	1520 (50%)	1397 (53%)
Unknown	36	598	506
Received (neo)adjuvant chemotherapy			
Yes	646 (51%)	1643 (54%)	1296 (49%)
No	630 (49%)	1423 (46%)	1347 (51%)
Assigned treatment			
Tamoxifen alone	441 (35%)	1021 (33%)	885 (33%)
Tamoxifen plus ovarian function suppression	415 (33%)	1024 (33%)	884 (33%)
Exemestane plus ovarian function suppression	420 (33%)	1021 (33%)	874 (33%)

Supplementary Table 2 - Clinicopathological characteristics of the SOFT combined sequencing cohort (N=1,276). Tumour grade, estrogen receptor expression, progesterone receptor expression and Ki-67 expression was centrally determined if tumour tissue was available, and locally determined otherwise.

Supplementary Table 3

Clinical characteristics of the young-age, matched case-control subsample (N=82)	
Age at enrolment	
< 35 years	22 (27%)
35 - 39 years	26 (32%)
40 - 44 years	34 (41%)
Tumour size	
≤ 2 cm	22 (27%)
> 2 cm	60 (73%)
Lymph node status	
Positive	60 (73%)
Negative	22 (27%)
Tumour grade	
One	7 (9%)
Two	44 (54%)
Three	31 (38%)
Estrogen receptor expression	
≥ 90%	56 (68%)
< 90%	26 (32%)
Progesterone receptor expression	
≥ 20%	61 (74%)
< 20%	21 (26%)
Ki-67 expression	
≥ 20%	46 (56%)
< 20%	33 (40%)
Received (neo)adjuvant chemotherapy	
Yes	74 (90%)
No	8 (10%)
Assigned treatment	
Tamoxifen alone	30 (37%)
Tamoxifen plus ovarian function suppression	29 (35%)
Exemestane plus ovarian function suppression	23 (28%)

Supplementary Table 3 - Clinicopathological characteristics of the young-age, matched case-control subsample (N=82). Tumour grade, estrogen receptor expression, progesterone receptor expression and Ki-67 expression was centrally determined if tumour tissue was available, and locally determined otherwise.

Supplementary Figure 2

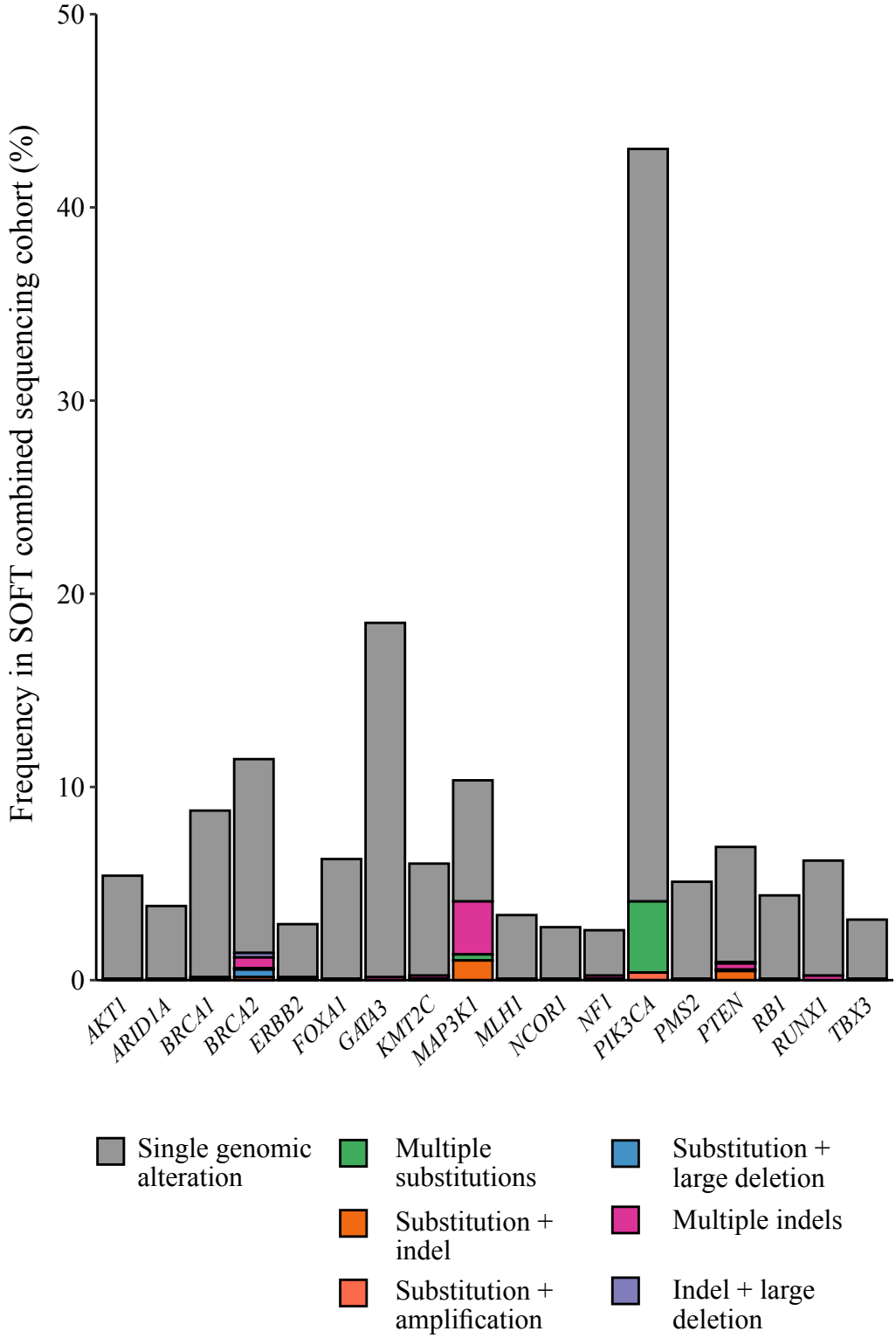

Supplementary Figure 2 - Bar plot demonstrating the presence and type of multiple genomic alterations in genes in individual patients in the SOFT combined sequencing cohort (N=1,276).

Supplementary Figure 3

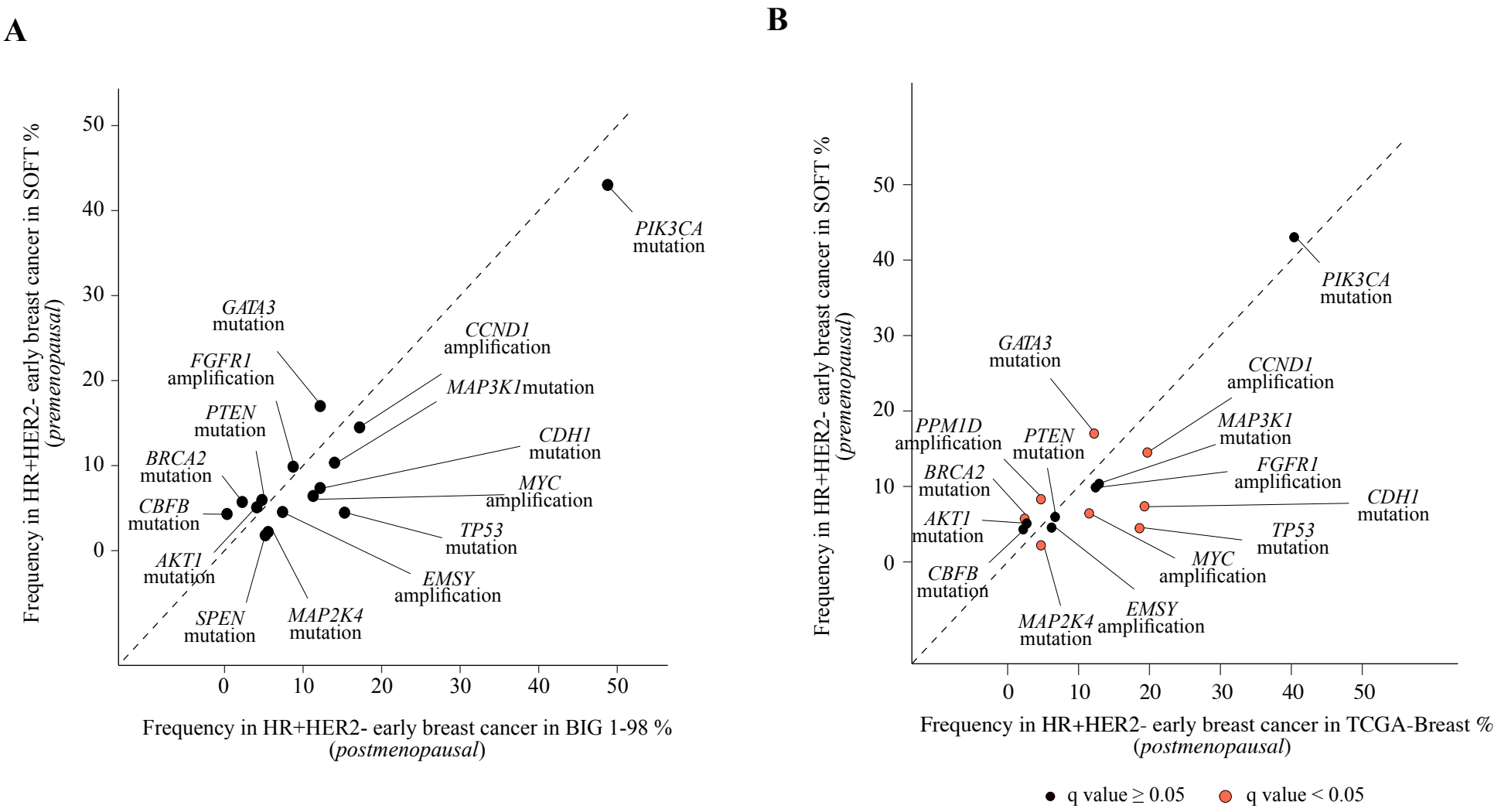

Supplementary Figure 3 - A comparison of the genomic driver alteration frequencies of premenopausal patients with HR+HER2- early breast cancer from the SOFT combined sequencing cohort (N=1,276) compared with postmenopausal patients with HR+HER2- early breast cancer from an analysis of the BIG 1-98 clinical trial (panel A, N=538), and the TCGA-Breast dataset (panel B, N=451). The dotted line provides demonstration of the plot points that represent equal frequencies between the groups.

Supplementary Table 4

Association of driver alterations with overall survival					
Genomic alteration	Number	Deaths	Hazard ratio (altered vs non-altered)	95% confidence interval	*P* value
PIK3CA mutation	549	33	0.91	0.59 - 1.40	0.665
GATA3 mutation	217	15	1.00	0.58 - 1.74	0.993
BRCA2 mutation	73	6	1.04	0.45 - 2.39	0.923
CDH1 mutation	94	7	0.88	0.41 - 1.90	0.746
TP53 mutation	57	5	1.05	0.42 - 2.58	0.921
FGFR1 amplification	126	20	1.94	1.18 - 3.20	0.009
MYC amplification	82	16	2.15	1.25 - 3.70	0.006
CCND1 amplification	185	30	2.15	1.39 - 3.33	0.001
PAK1 amplification	77	12	1.52	0.83 - 2.80	0.178
EMSY amplification	58	9	1.43	0.72 - 2.85	0.312
FOXA1 amplification	50	6	1.36	0.59 - 3.13	0.469
PPM1D amplification	106	16	1.46	0.85 - 2.52	0.170

Supplementary Table 4 - Association of driver alterations with overall survival comparing patients with tumours that harbour the driver alteration compared with patients with tumours that do not harbour the driver alteration in the SOFT combined sequencing cohort (N=1,276). Only driver alterations with ≥ 5 events are included.

Supplementary Table 5

A

Association of copy number altered subgroup with distant recurrence-free interval					
Copy number altered subgroup	Number	Distant recurrences	Hazard ratio (vs amplification-devoid)	95% confidence interval	*P* value
8q24 amplification (IntClust 9-like)	92	20	2.10	1.26 - 3.51	0.005
8p12 amplification (IntClust 6-like)	127	20	1.73	1.03 - 2.89	0.034
17q23 amplification (IntClust 1-like)	112	20	1.50	0.90 - 2.50	0.122
11q13 amplification (IntClust 2-like)	202	41	2.24	1.49 - 3.35	< 0.001

B

Association of copy number altered subgroup with overall survival					
Copy number altered subgroup	Number	Deaths	Hazard ratio (vs amplification-devoid)	95% confidence interval	*P* value
8q24 amplification (IntClust 9-like)	92	18	2.86	1.62 - 5.05	< 0.001
8p12 amplification (IntClust 6-like)	127	20	2.59	1.49 - 4.50	0.001
17q23 amplification (IntClust 1-like)	112	16	1.92	1.06 - 3.48	0.031
11q13 amplification (IntClust 2-like)	202	32	2.44	1.52 - 3.93	< 0.001

Supplementary Table 5 - Association of copy number altered subgroups with distant recurrence-free interval (Panel A) and overall survival (Panel B) comparing each copy number altered subgroup with the amplification-devoid subgroup in the SOFT combined sequencing cohort (N=1,276).

Supplementary Figure 4

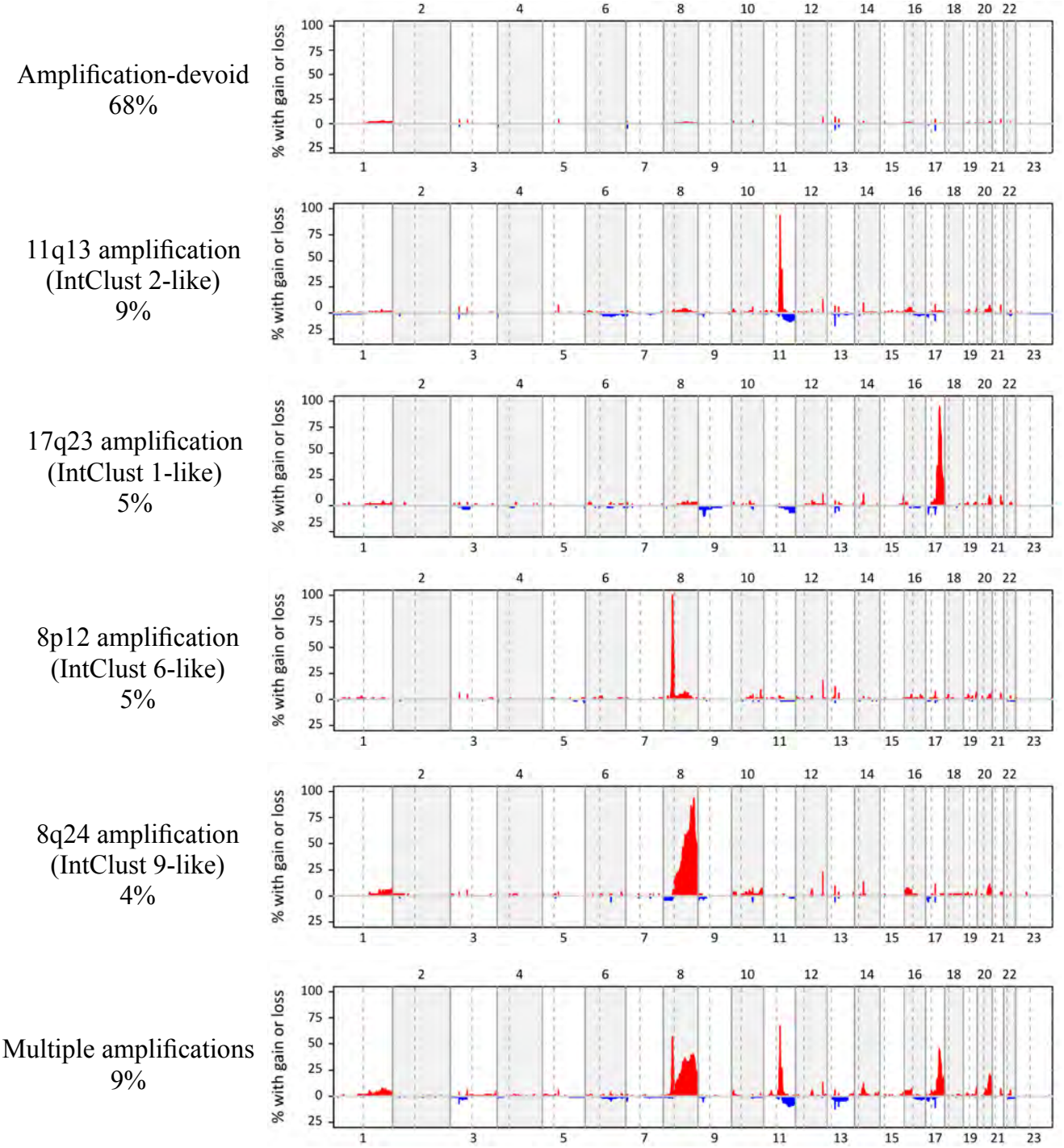

Supplementary Figure 4 - Genome wide copy number plots demonstrating proportion with gain (red) and loss (blue) in various genomic regions by each copy number altered subgroup in the SOFT combined sequencing cohort (N=1,276). Log ratio thresholds of 0.75 and -0.75 were utilised for this visualisation.

Supplementary Figure 5

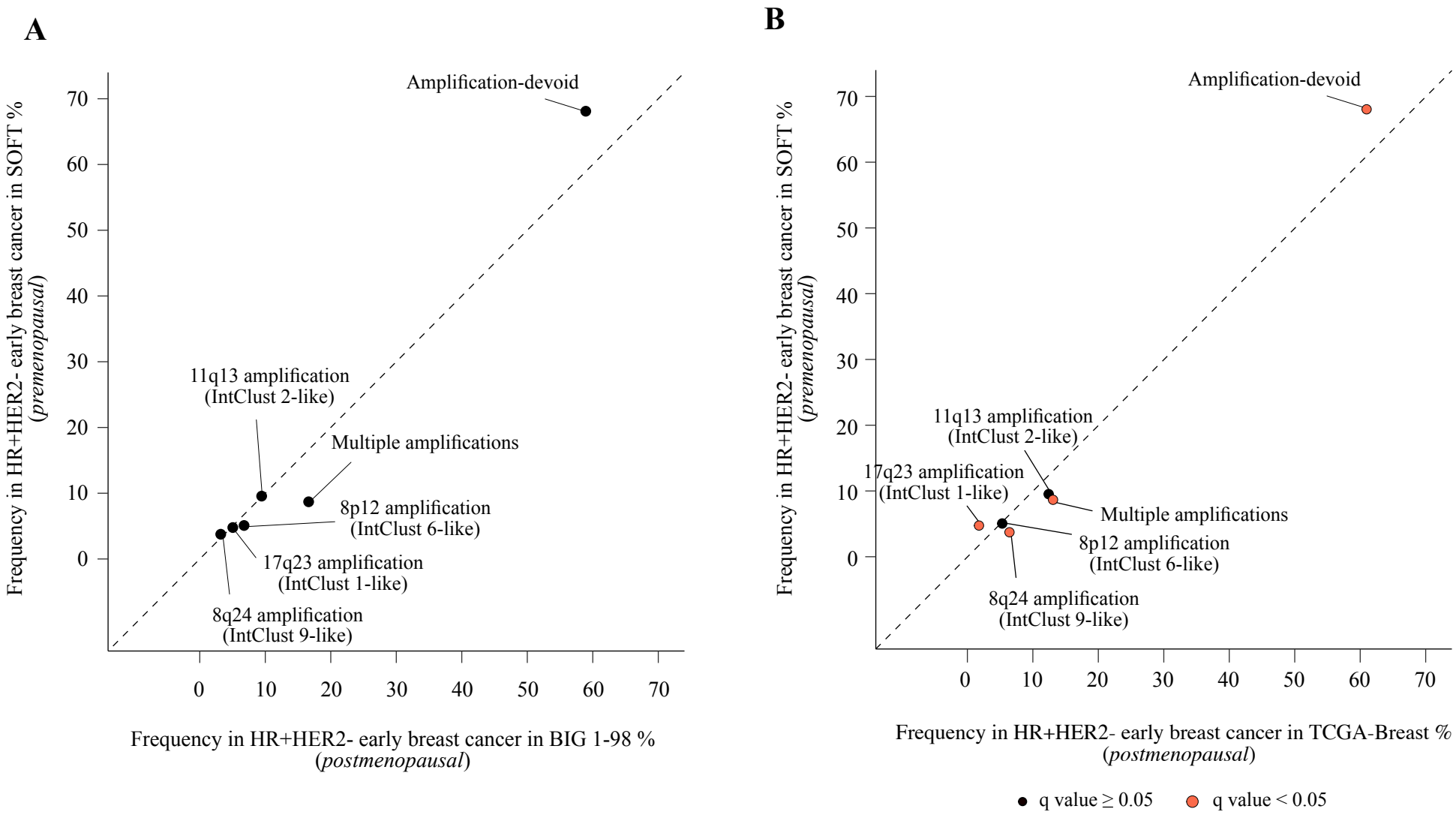

Supplementary Figure 5 - A comparison of the frequencies of copy number-amplified subgroups in premenopausal patients with HR+HER2- early breast cancer from the SOFT combined sequencing cohort (N=1,276) compared with postmenopausal patients with HR+HER2- early breast cancer from an analysis of the BIG 1-98 clinical trial (panel A, N=538) and the TCGA-Breast dataset (Panel B, N=451). The dotted line provides demonstration of the plot points that represent equal frequencies between the groups.

Supplementary Figure 6

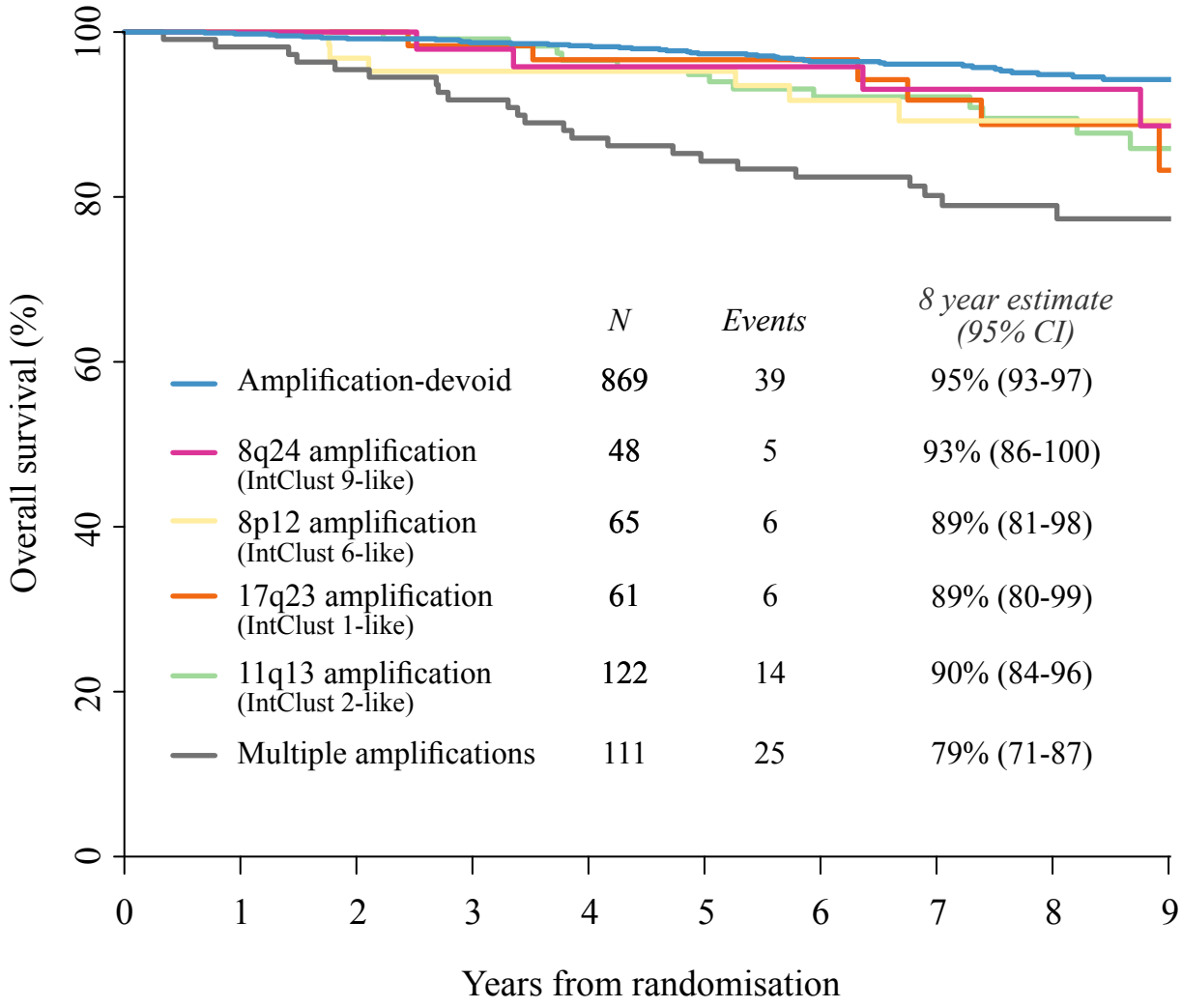

Supplementary Figure 6 - Kaplan-Meier plot estimating the overall survival based on the copy number altered subgroup in the SOFT combined sequencing cohort (N=1,276).

Supplementary Figure 7

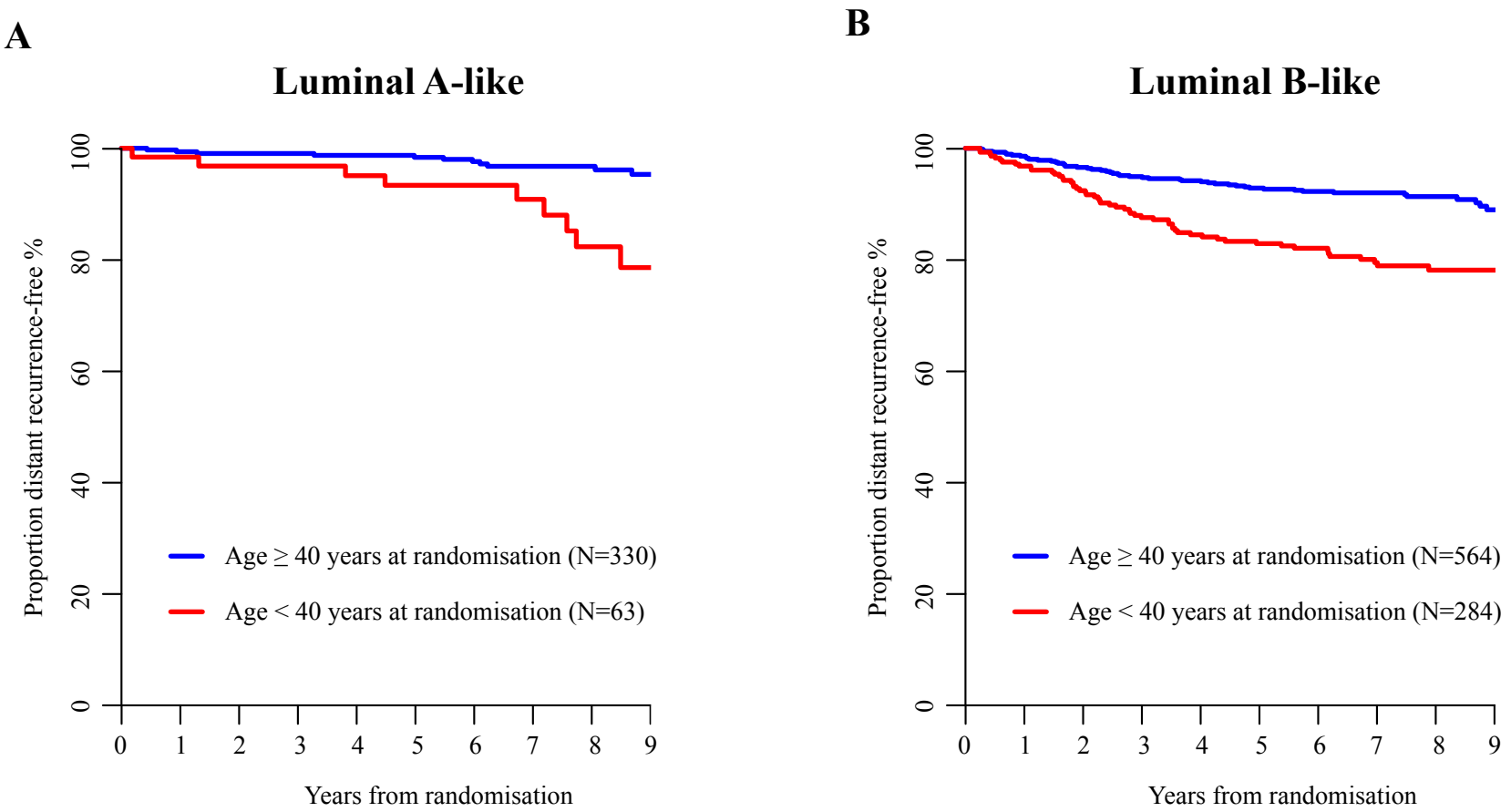

Supplementary Figure 7 - Kaplan Meier plots estimating the proportion distant recurrence-free in luminal A-like tumours (panel A) and luminal B-like tumours (panel B) based on the patient's age at randomisation in the SOFT combined sequencing cohort (N=1,276).

Supplementary Figure 8

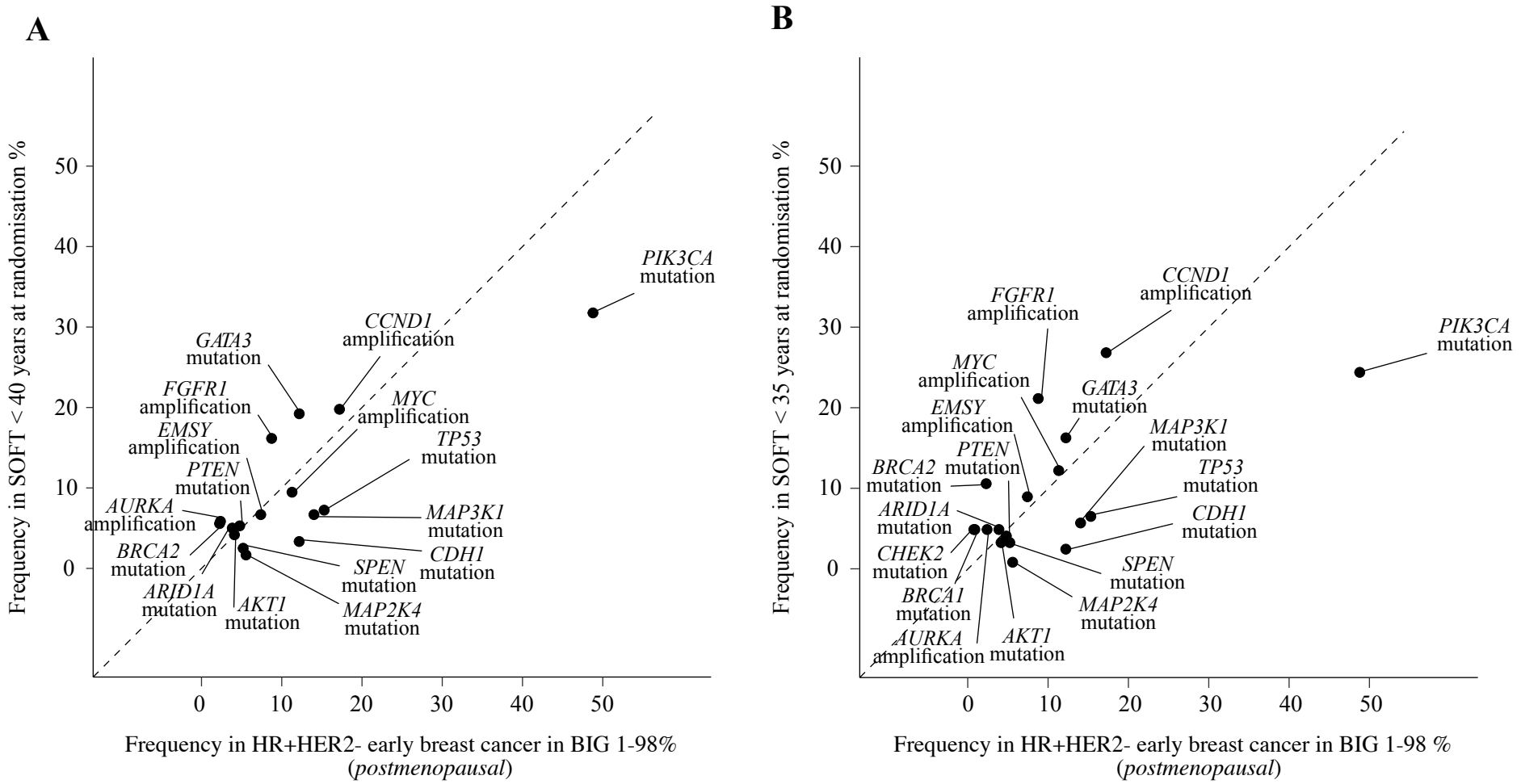

Supplementary Figure 8 - A comparison of the frequencies of genomic driver alterations in patients with HR+HER2- early breast cancer from the SOFT combined sequencing cohort compared with postmenopausal patients with HR+HER2- early breast cancer from an analysis of the BIG 1-98 clinical trial (N=538). Panel A compares patients from SOFT age < 40 at randomisation (N=359) and panel B compares patients from SOFT aged < 35 at randomisation (N=123). The dotted line provides demonstration of the plot points that represent equal frequencies between the groups.

Supplementary Figure 9

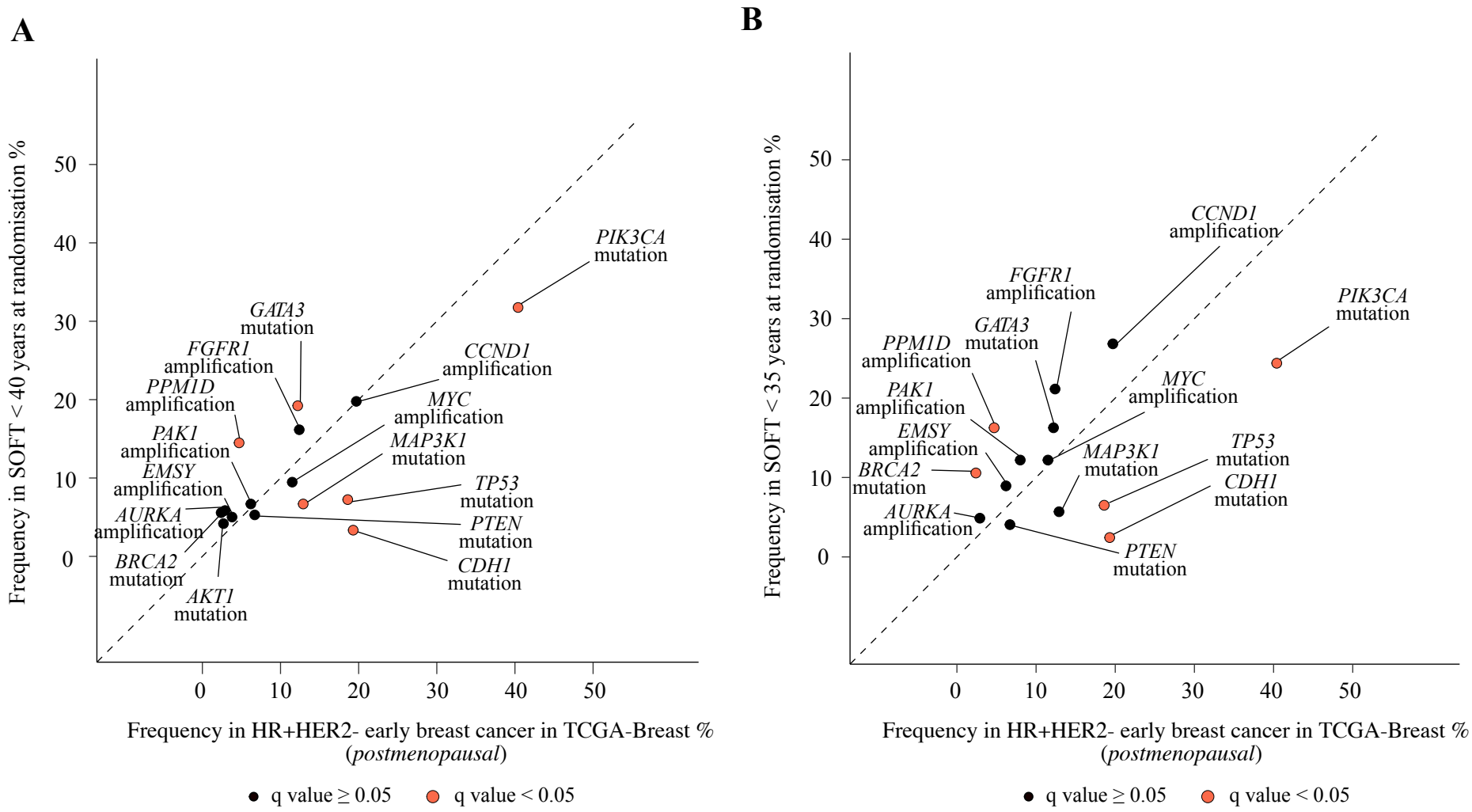

Supplementary Figure 9 - A comparison of the frequencies of genomic driver alterations in patients with HR+HER2- early breast cancer from the SOFT combined sequencing cohort compared with postmenopausal patients with HR+HER2- early breast cancer from the TCGA-Breast dataset (N=451). Panel A compares patients from SOFT age < 40 at randomisation (N=359) and panel B compares patients from SOFT aged < 35 at randomisation (N=123). The dotted line provides demonstration of the plot points that represent equal frequencies between the groups.

Supplementary Figure 10

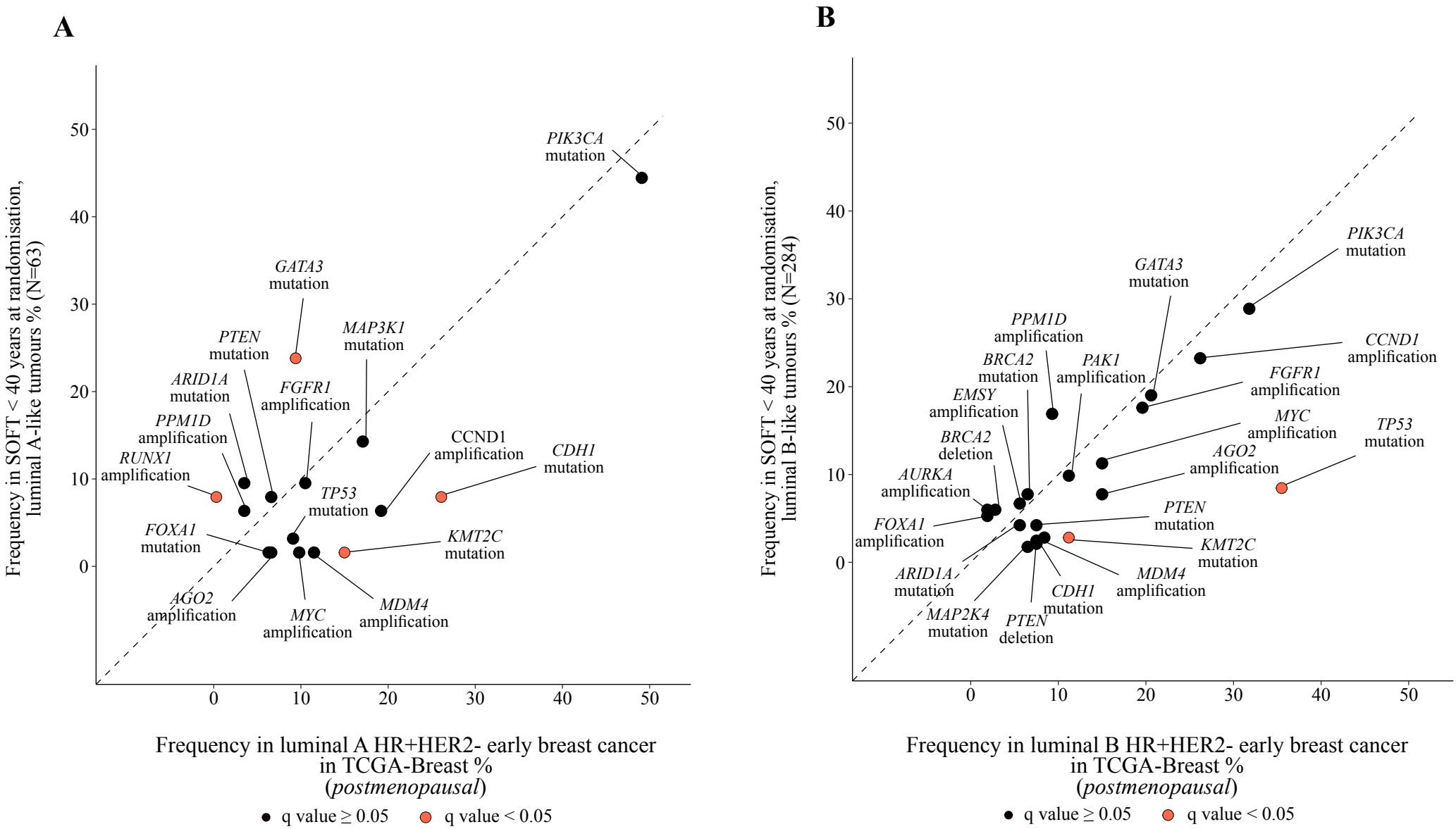

Supplementary Figure 10 - Panel A compares patients from SOFT age < 40 years at randomisation with luminal A-like tumours (N=63) with postmenopausal patients with luminal A HR+HER2- early breast cancer from the TCGA-Breast dataset (N=287). Panel B compares patients from SOFT age < 40 years at randomisation with luminal B-like tumours (N=284) with postmenopausal patients with luminal B HR+HER2- early breast cancer from the TCGA-Breast dataset (N=107). The dotted line provides demonstration of the plot points that represent equal frequencies between the groups.

Supplementary Figure 11

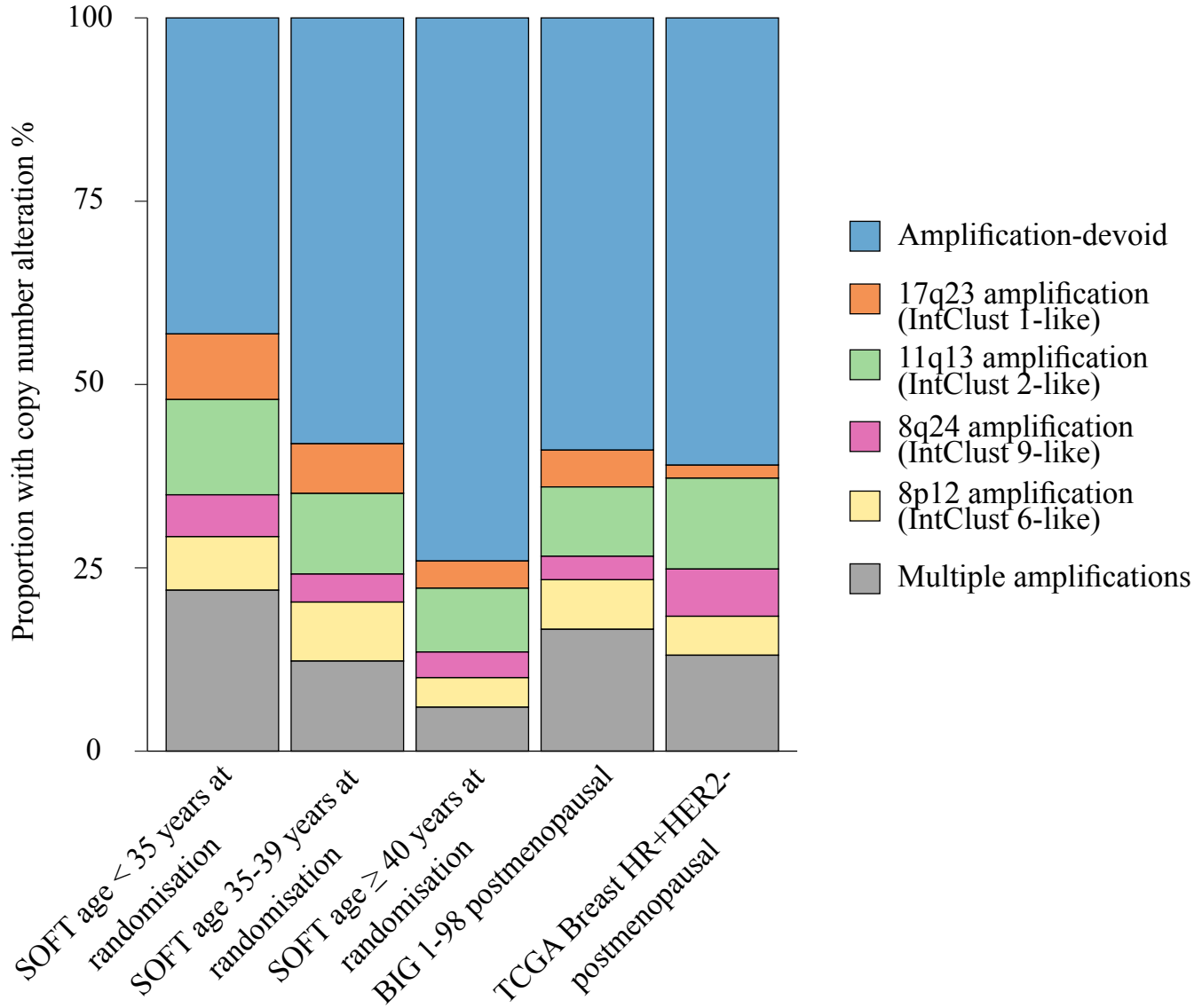

Supplementary Figure 11 - A comparison of the frequencies of copy number altered subgroups according to patients age at randomization in the SOFT combined sequencing cohort (N=1,276), and with postmenopausal women enrolled in BIG 1-98 (N=538), and with postmenopausal women with HR+HER2- breast cancer in the TCGA-Breast dataset (N=451).

Supplementary Figure 12

	Number	Frequency in patients with and without distant recurrence	Odds ratio for distant recurrence	95% confidence interval	P value
GATA3 mutation	22	24% vs 30%	0.7	0.27 - 1.84	0.472
PIK3CA mutation	20	19% vs 25%	0.74	0.25 - 2.18	0.588
CCND1 amplification	15	29% vs 8%	4.15	1.16 - 14.91	0.029
PPM1D amplification	15	21% vs 15%	1.36	0.41 - 4.51	0.613
FGFR1 amplification	14	17% vs 15%	1.2	0.37 - 3.93	0.763
DAXX deletion	10	12% vs 13%	0.8	0.21 - 3.01	0.736
MYC amplification	9	12% vs 10%	1.1	0.24 - 5.02	0.898
PAK1 amplification	9	17% vs 5%	3.65	0.72 - 18.35	0.117
TP53 deletion	9	12% vs 10%	1.22	0.26 - 5.66	0.797
AGO2 amplification	5	10% vs 3%	3.56	0.39 - 32.19	0.258
AURKA amplification	5	7% vs 5%	1.53	0.25 - 9.52	0.649
CDH1 mutation	5	7% vs 5%	2.56	0.23 - 29.12	0.448
FOXA1 amplification	5	7% vs 5%	1.53	0.25 - 9.52	0.649
TP53 mutation	5	5% vs 8%	0.76	0.12 - 4.61	0.764

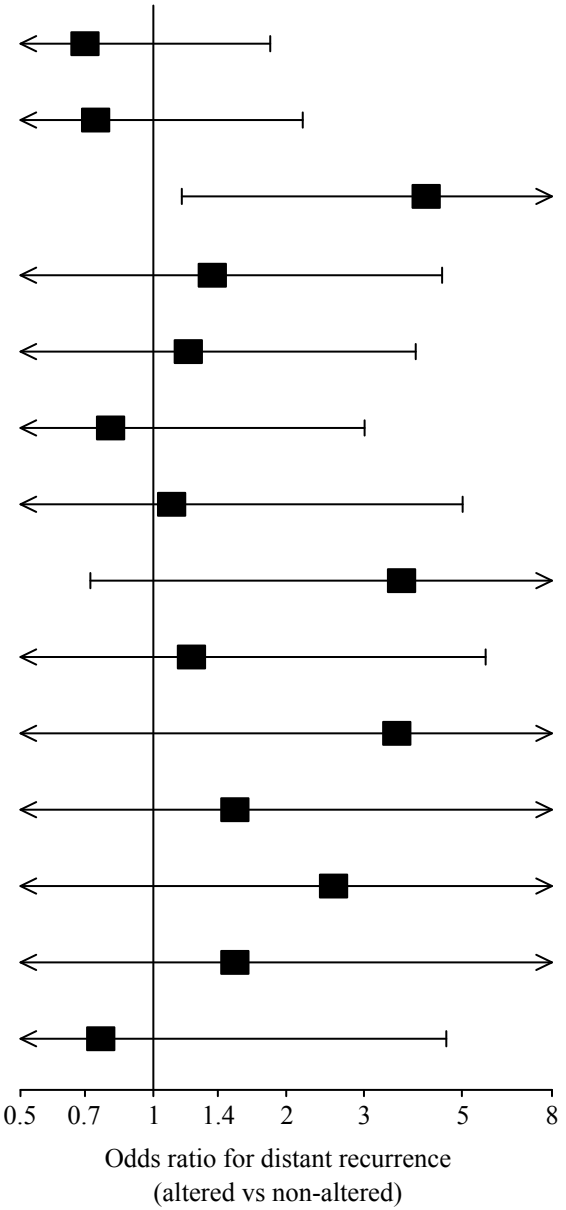

Supplementary Figure 12 - Association of driver alterations with distant recurrence in the young-age, case-control subsample that underwent WES (N=82) using a conditional logistic regression model, stratified by case-control matching.

Supplementary Figure 13

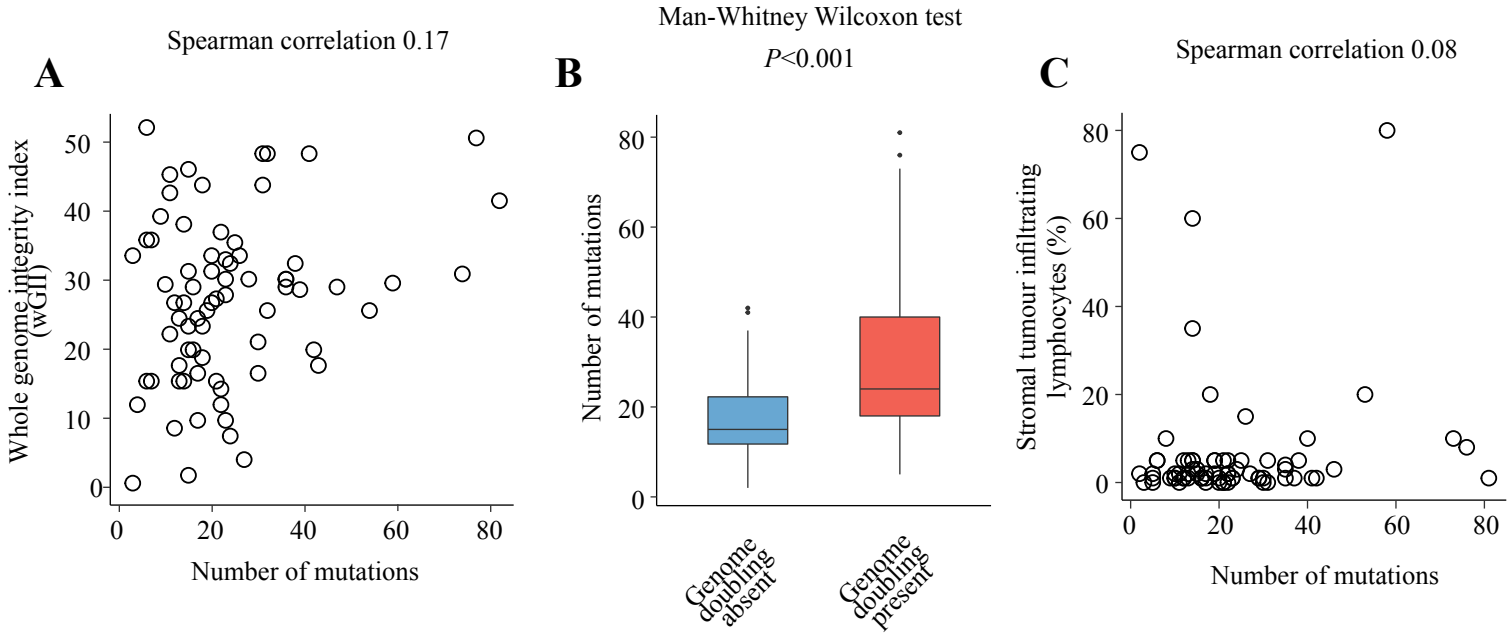

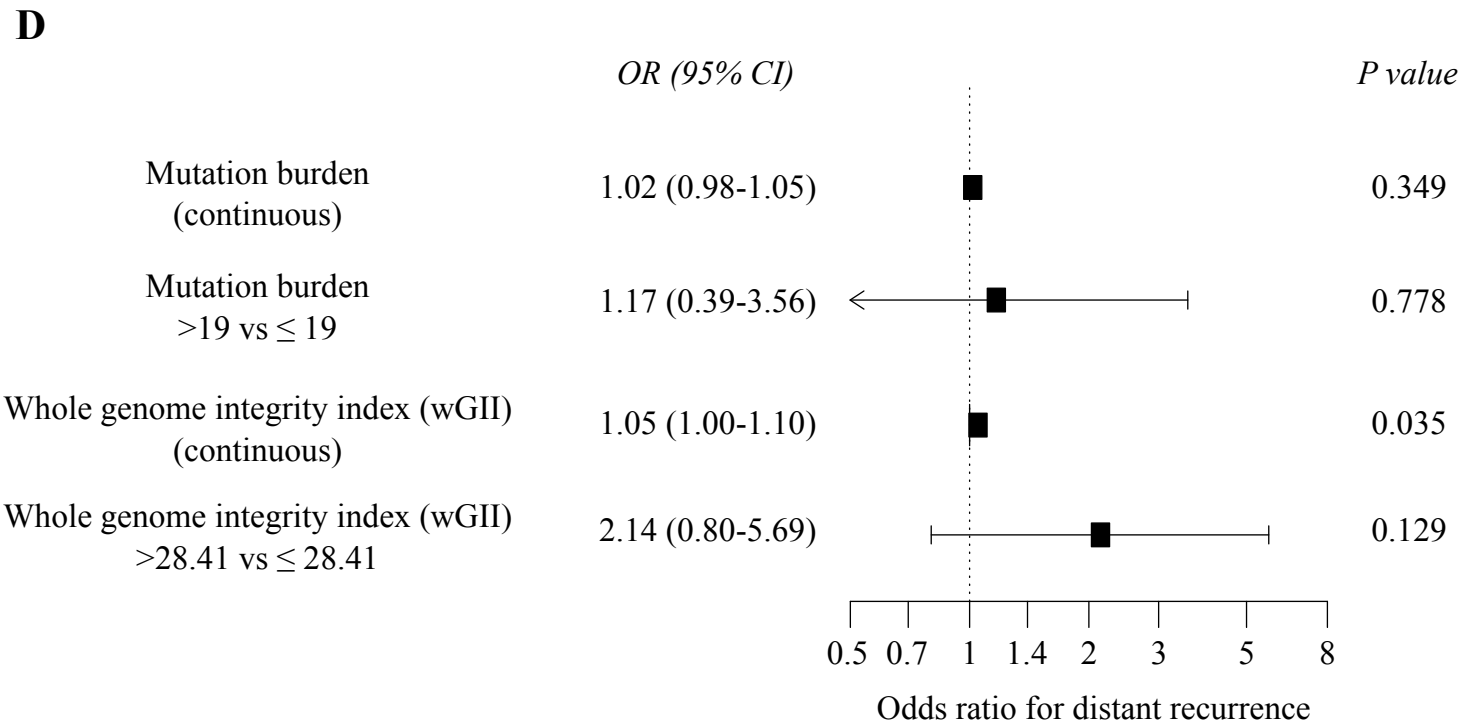

Supplementary Figure 13 - Plots demonstrating the relationship between number of mutations with the whole genome integrity index (wGII) (panel A), whole genome doubling (panel B), and quantities of stromal tumour infiltrating lymphocytes (panel C) in the SOFT matched case-control subsample that had paired tumour-normal whole exome sequencing (N=73). Panel D demonstrates the association of genomic features with risk of distant recurrence in the SOFT matched case-control subsample (N=82). Cut-off values for mutation burden and whole genome integrity index were arbitrarily defined using the median. Abbreviations: OR, odds ratio; 95% CI, 95% confidence interval.

Supplementary Figure 14

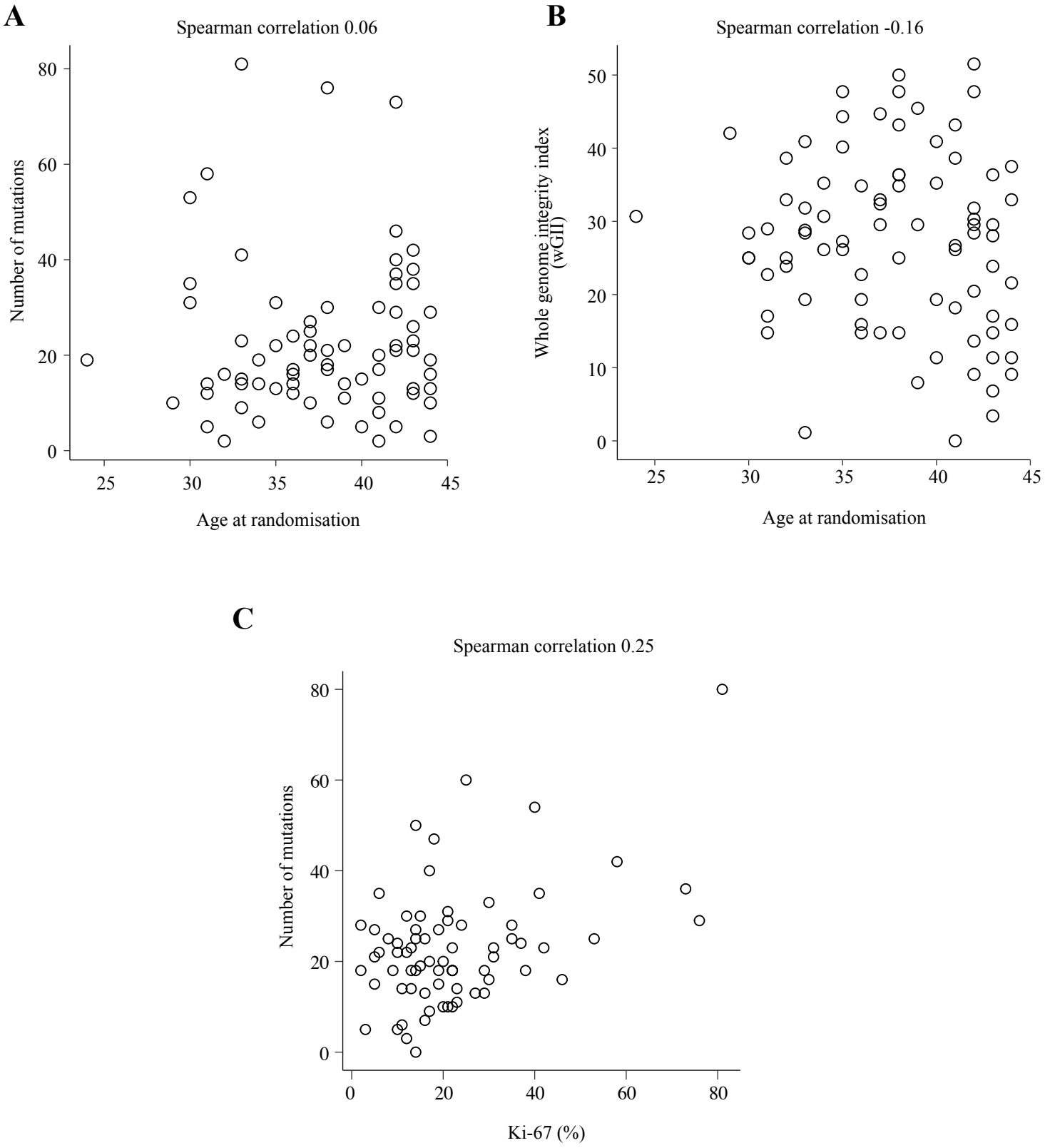

Supplementary Figure 14 - Plots demonstrating the relationship between age at randomisation with number of mutations (panel A), age at randomisation with the whole genome integrity index (wGII) (panel B), and number of mutations with Ki-67 (%) levels (Panel C) in the SOFT matched case-control subsample that had paired tumour-normal whole exome sequencing (N=73).

Supplementary Figure 15

A

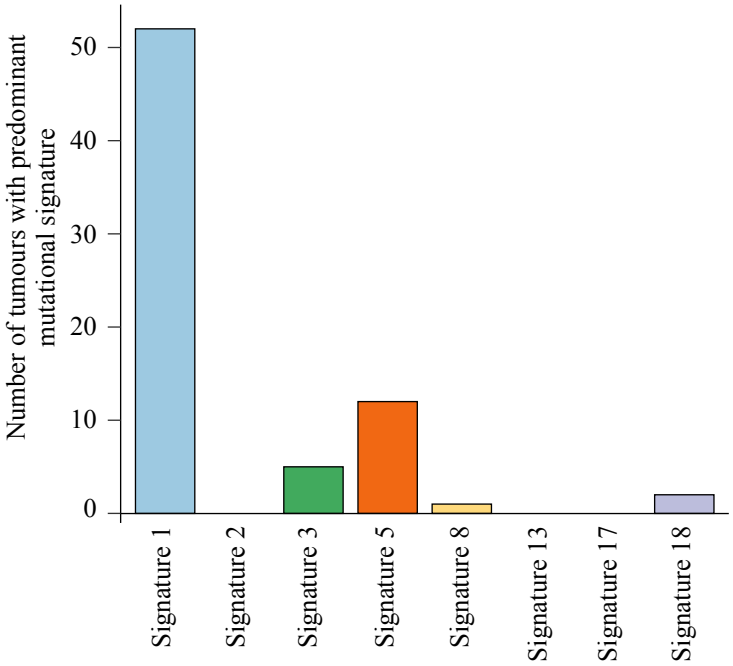

B

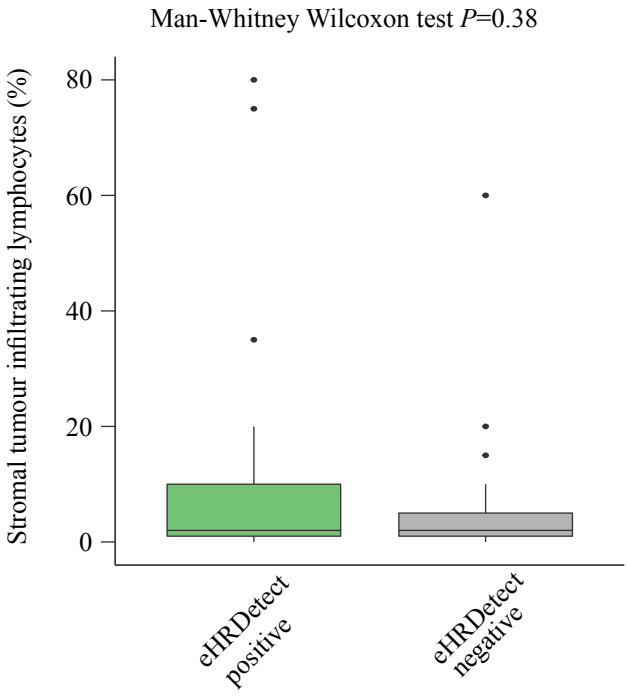

C

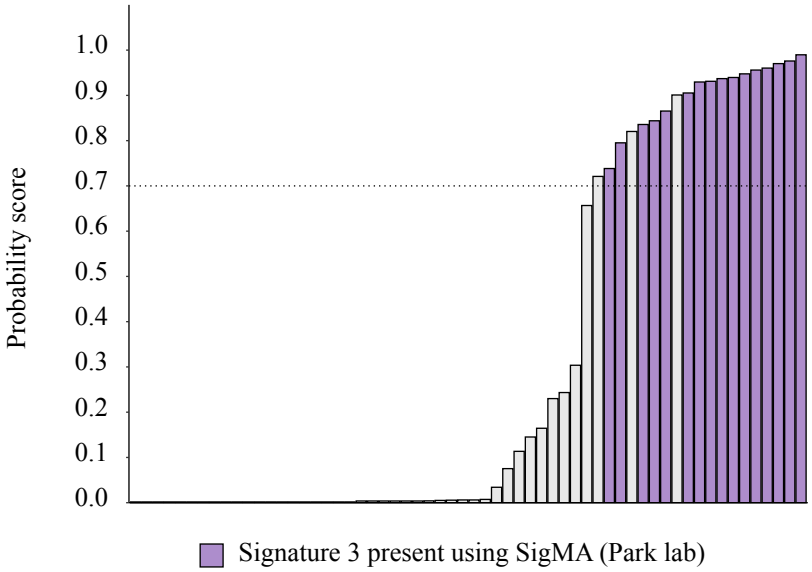

D

		SigMA signature 3	
		Negative	Positive
eHRDetect	Negative	41	0
	Positive	3	16

Supplementary Figure 15 - Results from the SOFT matched case-control subsample that had paired tumour-normal whole exome sequencing (N=73). Panel A demonstrates the frequency of tumours with each respective predominant mutational signature. The predominant mutational signature was defined as the mutational signature that was most prevalent in the tumour. Panel B demonstrates the quantity of stromal tumour infiltrating lymphocytes by eHRDetect status in the matched case-control subsample that was evaluable for eHRDetect (N=68). Panel C demonstrates the eHRDetect probability score and presence of mutational signature 3 using SigMA in patients who were evauble for both eHRDetect and SigMA (N=60). Panel D demonstrates the number of patients with positive or negative scores using eHRDetect and SigMA.

Supplementary Figure 16

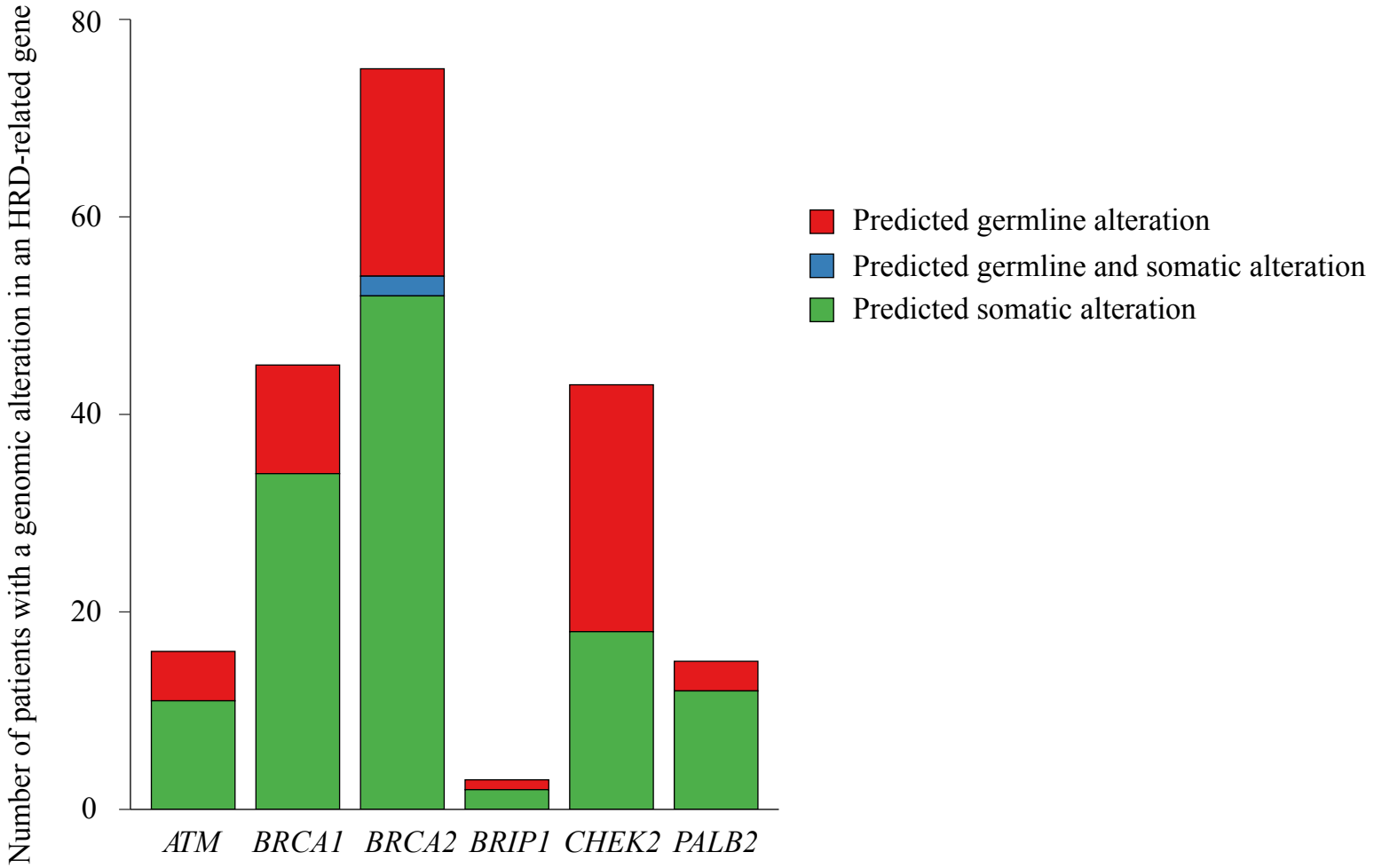

Supplementary Figure 16 - Bar plot demonstrating the number of patients with HRD-related genomic alterations. Alterations were predicted to be germliine if they were known to be pathogenic in ClinVar and had a variant allele frequency > 0.45.

Supplementary Table 6

Associations with distant recurrence-free interval in premenopausal women aged < 40 years and ≥ 40 years at randomisation							
	Age < 40 years at randomisation			Age ≥ 40 years at randomisation			Interaction *P* value
Genomic alteration	Number of very young women	Events	Hazard ratio and 95% confidence interval (altered vs non-altered)	Number of young women	Events	Hazard ratio and 95% confidence interval (altered vs non-altered)	
PIK3CA mutation	114	26	1.78 (1.08 - 2.92)	435	19	0.58 (0.33 - 0.99)	0.002
GATA3 mutation	69	17	1.47 (0.85 - 2.54)	148	6	0.66 (0.28 - 1.53)	0.140
CDH1 mutation	12	0	NE	82	7	1.04 (0.47 - 2.30)	0.995
KMT2C mutation	9	0	NE	68	5	1.09 (0.44 - 2.73)	0.994
TP53 mutation	26	3	0.56 (0.18 - 1.79)	31	5	2.40 (0.95 - 6.06)	0.061
FGFR1 amplification	58	14	1.29 (0.71 - 2.32)	68	6	1.14 (0.48 - 2.66)	0.819
MYC amplification	34	10	1.62 (0.82 - 3.17)	48	7	1.63 (0.73 - 3.62)	0.957
CCND1 amplification	71	24	2.21 (1.33 - 3.65)	114	14	1.80 (0.99 - 3.29)	0.538
PAK1 amplification	30	9	1.20 (0.59 - 2.44)	47	7	2.33 (1.06 - 5.16)	0.241
EMSY amplification	24	7	1.06 (0.48 - 2.34)	34	5	2.24 (0.89 - 5.61)	0.260
PPM1D amplification	52	11	0.88 (0.46 - 1.70)	54	9	1.74 (0.85 - 3.55)	0.194

Supplementary Table 6 - Association of driver alterations with distant recurrence-free interval in very young women (aged < 40 years at randomisation) compared with in young women (aged ≥ 40 years at randomisation) in the SOFT combined sequencing cohort (N=1,276). The Interaction P value is derived from the product interaction term in the Cox proportional hazards regression model.

Supplementary Figure 17

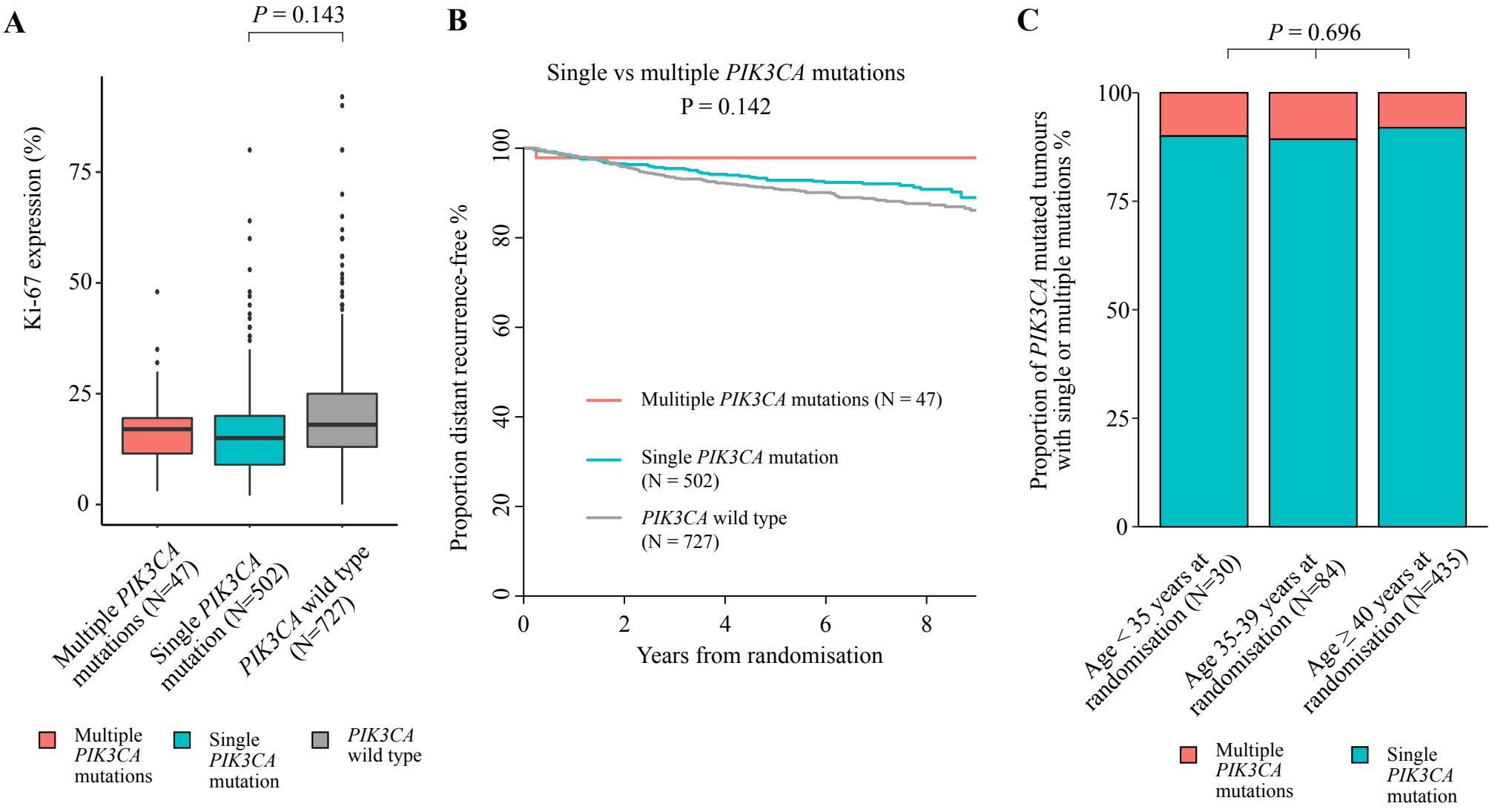

Supplementary Figure 17 - Plots demonstrating the association of multiple *PIK3CA* mutations with ki-67 expression levels (panel A), distant recurrence-free interval (panel B), and age at randomisation (panel C) in the SOFT combined sequencing cohort (N=1,276).

Supplementary Figure 18

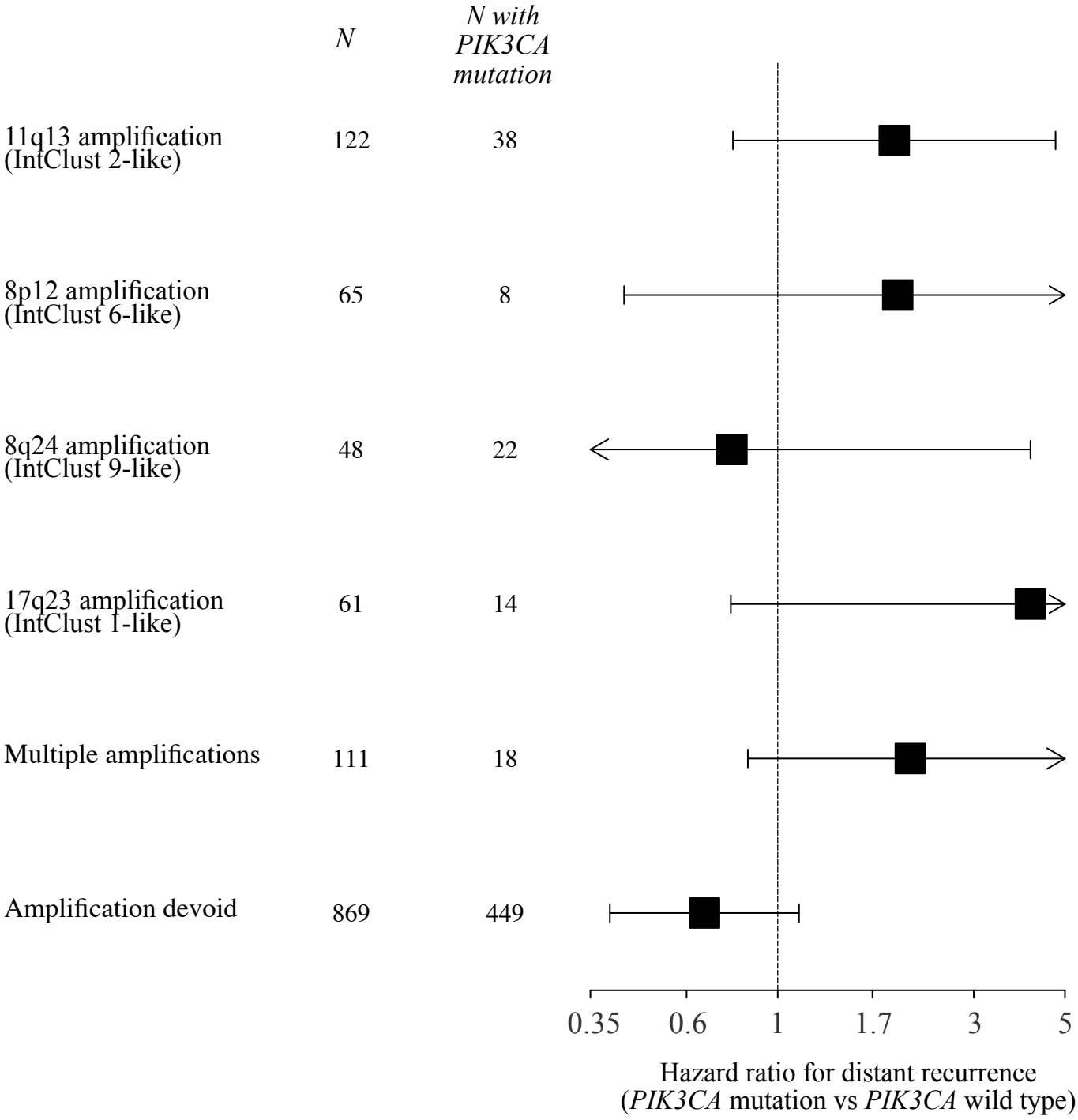

Supplementary Figure 18 - Forest plot demonstrating the hazard ratio for distant recurrence across the copy number alteration subgroups. Abbreviations: N, number.

Supplementary Figure 19

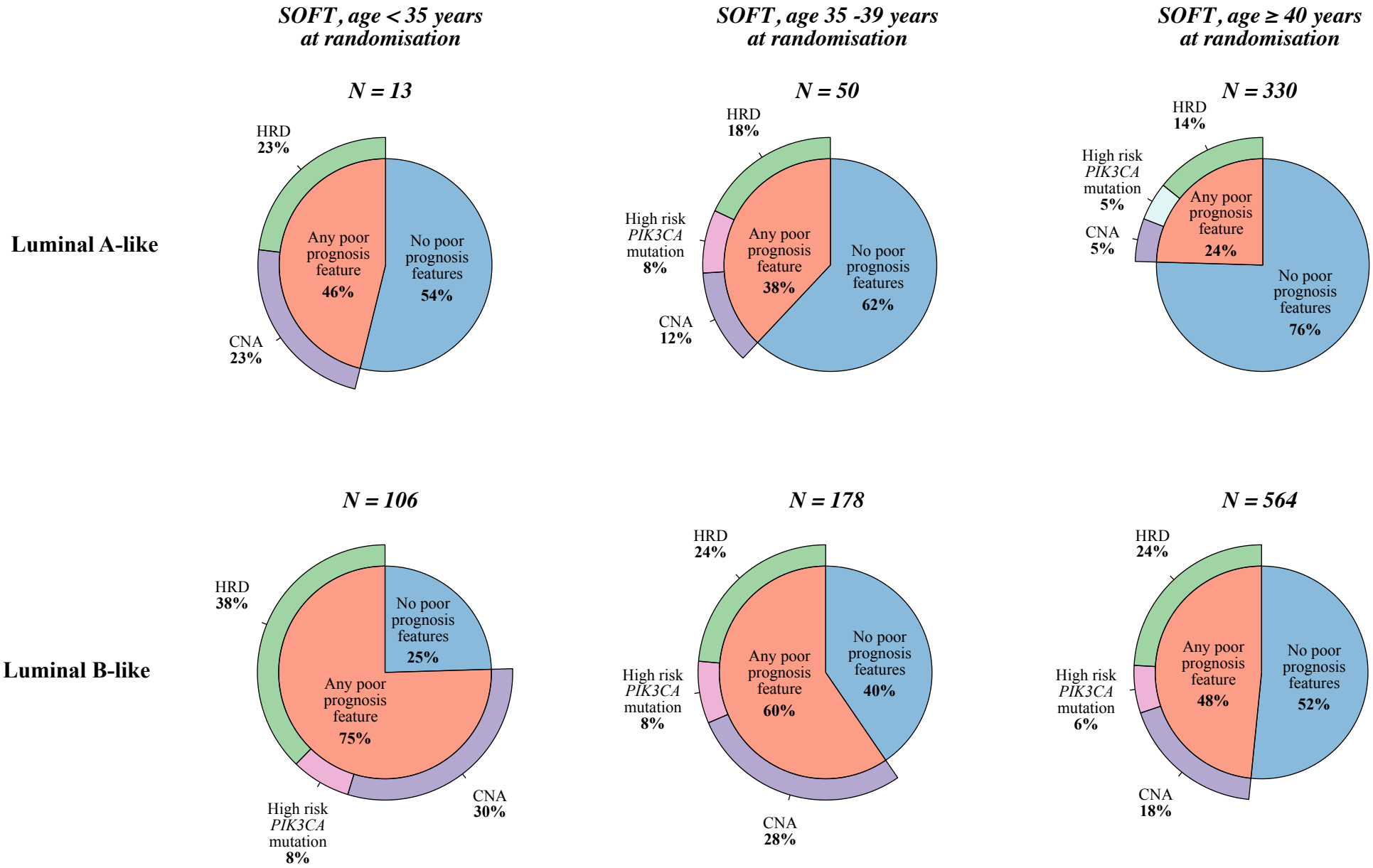

Supplementary Figure 19 - Pie charts demonstrating the frequencies of prognostic genomic features in the SOFT combined sequencing cohort (N=1,276), based on the proposed framework for tumour subgrouping, and according to age at randomisation. Tumours are further subgrouped into luminal A-like tumours (top panel) and luminal B-like tumours (bottom panel)

Supplementary Figure 20

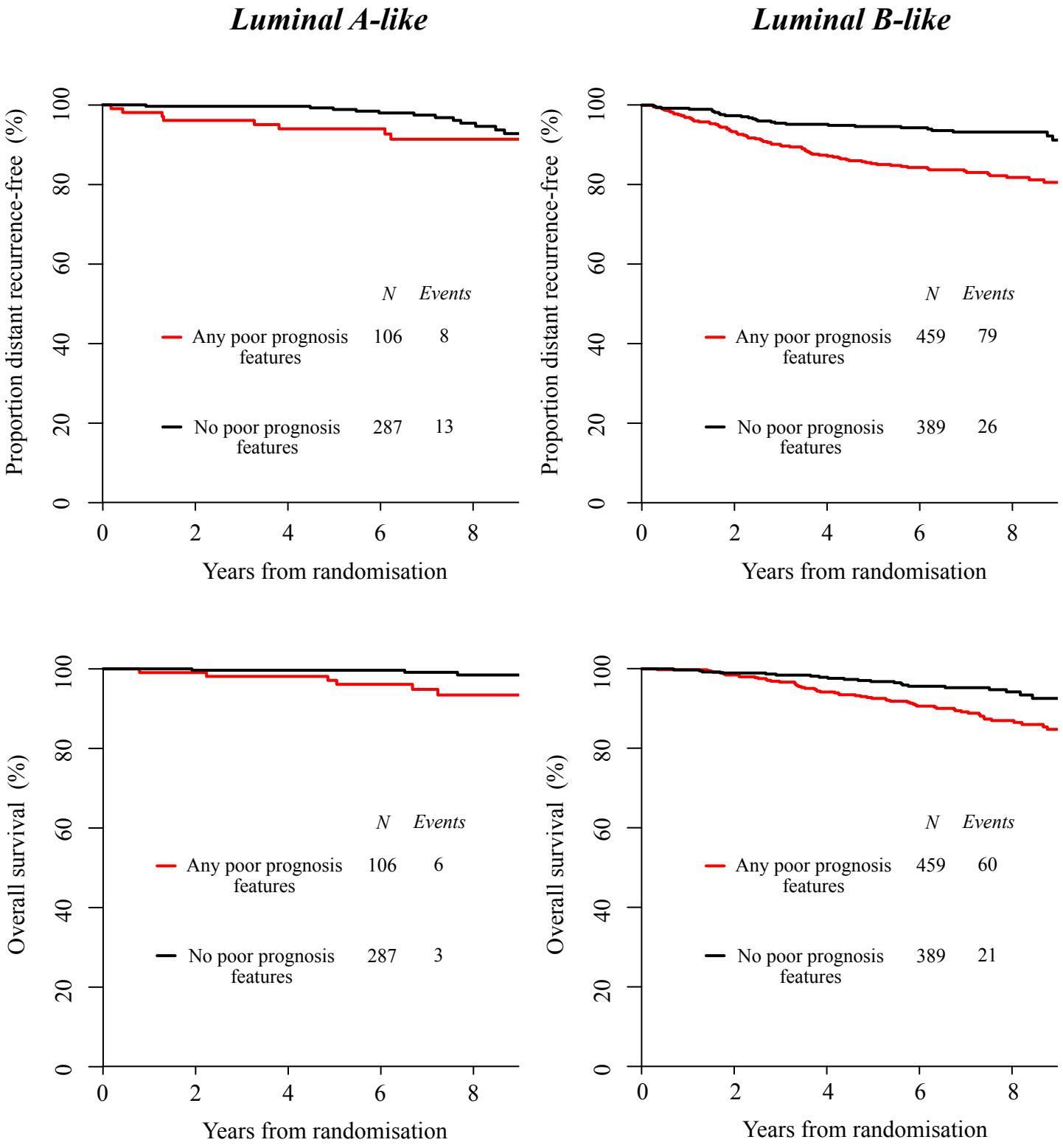

Supplementary Figure 20 - Kaplan Meier curves estimating the proportion distant-recurrence free (top panels) and overall survival (bottom panels) in patients that have tumours with a luminal A-like phenotype (left panels) and luminal B-like phenotype (right panels) in the SOFT combined sequencing cohort (N=1,276). Any poor prognosis features includes tumours that are classified as HRD, high risk *PIK3CA* mutation, or CNA. Abbreviations: HRD, homologous recombination deficiency; CNA, copy number-amplified.

Supplementary Table 7

Distant recurrence free-interval		
	Likelihood ratio test Chi-squared value	**Likelihood ratio test *P* value**
Model 1 - Stratified by nodal status and chemotherapy receipt, adjusted by luminal-like status, treatment assignment, age, **AND genomic subgrouping**	11.11	0.011
Model 2 - Stratified by nodal status and chemotherapy receipt, adjusted by luminal-like status, treatment assignment, and age		

Overall survival		
	Likelihood ratio test Chi-squared value	**Likelihood ratio test *P* value**
Model 1 - Stratified by nodal status and chemotherapy receipt, adjusted by luminal-like status, treatment assignment, age, **AND genomic subgrouping**	10.38	0.016
Model 2 - Stratified by nodal status and chemotherapy receipt, adjusted by luminal-like status, treatment assignment, and age		

Supplementary Table 7 - Tables demonstrating Likelibood ratio test Chi-squared values and *P* values for Cox Proportional Hazard Regression Models using the described variables to demonstrate the added prognostic value of genomic subgrouping in the SOFT combined sequencing cohort (N=1,276). The genomic subgrouping was as described (no poor prognosis feature / HRD / high risk *PIK3CA* mutation / CNA). Abbreviations: HRD, homologous recombination deficiency; CNA, copy number amplified.

Supplementary Figure 21

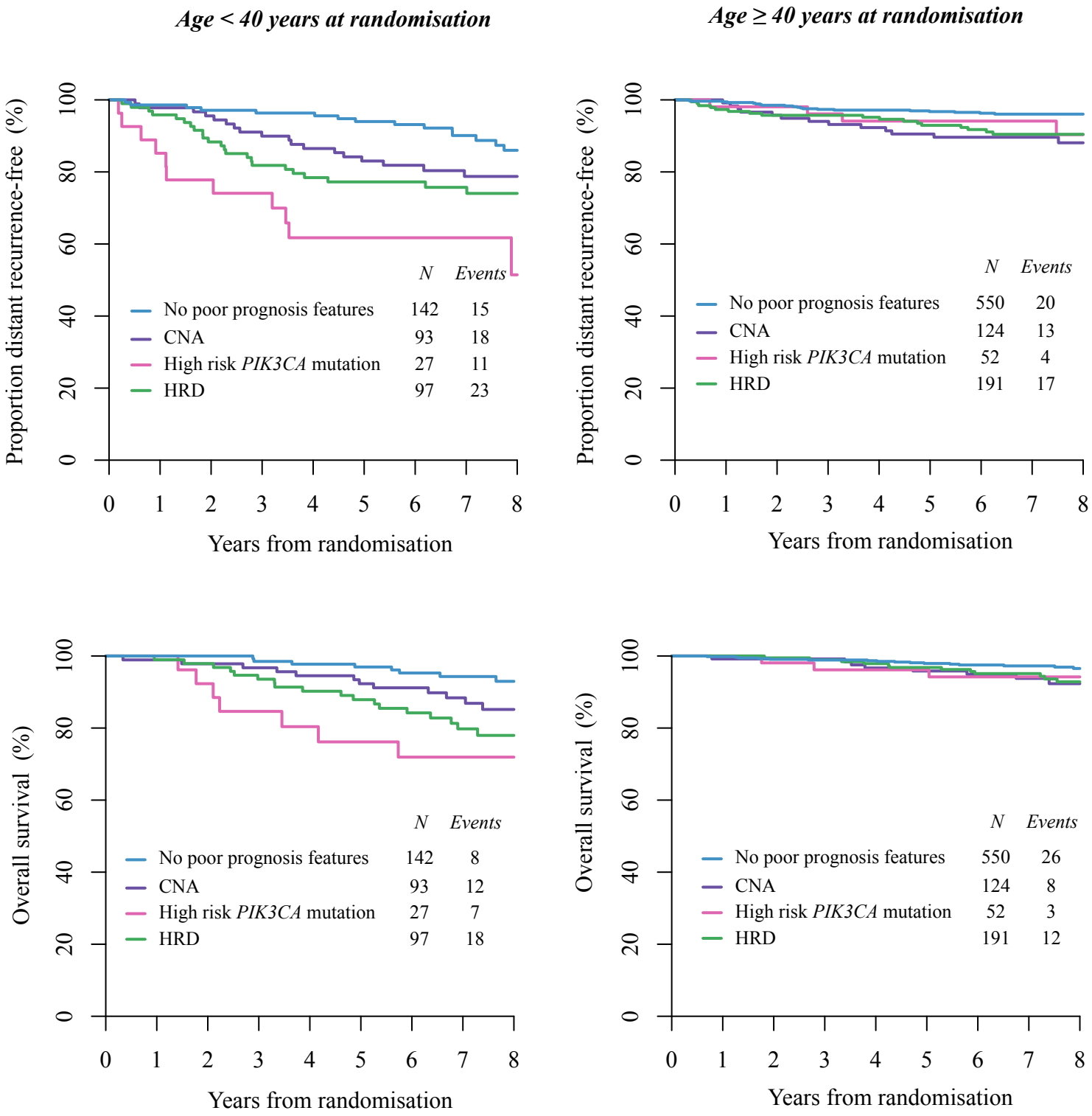

Supplementary Figure 21 - Kaplan Meier curves estimating the proportion distant-recurrence free (top panels) and overall survival (bottom panels) in patients age < 40 years at randomisation (left panels) and age ≥ 40 years at randomisation (right panels) in the SOFT combined sequencing cohort (N=1,276) by genomic subgrouping. Abbreviations: HRD, homologous recombination deficiency; CNA, copy number-amplified.

Supplementary Figure 22

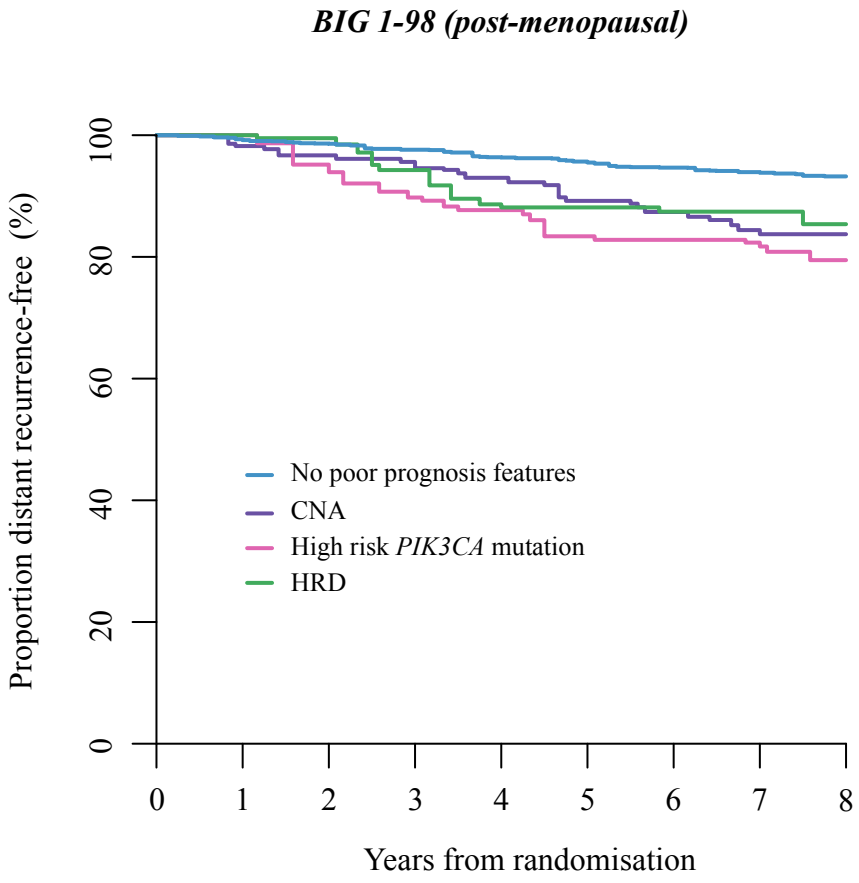

Supplementary Figure 22 - Kaplan Meier curves estimating the proportion distant-recurrence free in patients from the post-menopausal BIG 1-98 cohort by genomic subgrouping. Abbreviations: HRD, homologous recombination deficiency; CNA, copy number-amplified.

Supplementary Figure 23

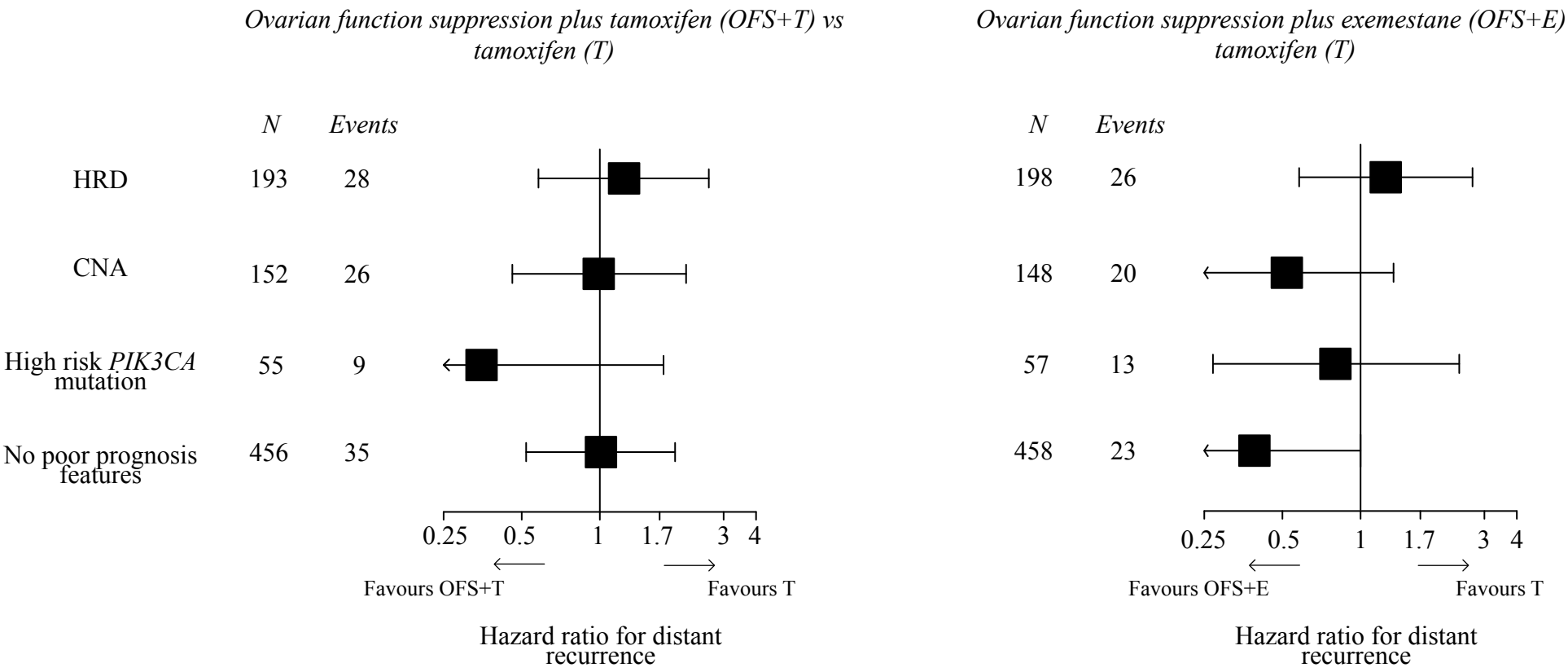

Supplementary Figure 23 - Forest plots demonstrating treatment associations in the SOFT combined sequencing cohort (N=1,276). Hazard ratio estimates (boxes) and 95% confidence intervals (lines) derived from Cox proportional hazard regression models comparing patients assigned various endocrine treatment, subgrouped by prognostic genomic features. Abbreviations: HRD, homologous recombination deficiency; CNA, copy number-amplified; OFS, ovarian function supression; T, tamoxifen; E, exemestane.